CHAPTER 6

TURN PERFORMANCE AND AGILITY

CHAPTER 6

TURN PERFORMANCE AND AGILITY

CHAPTER 6

FIGURES

CHAPTER 6

EQUATIONS

$\omega = \frac{V_T}{R}$	(Eq 6.13)	6.6
$\omega = \frac{g}{V_T} \tan\phi$	(Eq 6.14)	6.6
$\omega = \frac{g}{V_T} \sqrt{\left(n_z^2 - 1\right)}$	(Eq 6.15)	6.6
$\phi = \tan^{-1}\left(\frac{F_Y}{W}\right)$	(Eq 6.16)	6.8
$L = \frac{W}{\cos\phi}$	(Eq 6.17)	6.8
$\Delta L = F_Y \tan\phi$	(Eq 6.18)	6.9
$F_R = W\tan\phi + \frac{F_Y}{\cos\phi}$	(Eq 6.19)	6.10
$n_R = \tan\phi + \frac{n_Y}{\cos\phi}$	(Eq 6.20)	6.10
$\phi_E = \tan^{-1}\left(\tan\phi + \frac{n_Y}{\cos\phi}\right)$	(Eq 6.21)	6.10
$R = \frac{V_T^2}{g\left(\tan\phi + \frac{n_Y}{\cos\phi}\right)}$	(Eq 6.22)	6.10
$\omega = \frac{g\left(\tan\phi + \frac{n_Y}{\cos\phi}\right)}{V_T}$	(Eq 6.23)	6.10
$\Delta\omega = \frac{g\, n_Y}{V_T \cos\phi}$	(Eq 6.24)	6.10
$n_R = n_z - \cos\gamma$	(Eq 6.25)	6.12

$$R_{(\text{wings level})} = \frac{V_T^2}{g\,(n_z - \cos\gamma)}$$ (Eq 6.26) 6.12

$$\omega_{(\text{wings level})} = \frac{g\,(n_z - \cos\gamma)}{V_T}$$ (Eq 6.27) 6.12

$$L = C_L q S + T_G \sin\alpha_j$$ (Eq 6.28) 6.16

$$n_z = \frac{C_L q}{W/S} + \frac{T_G}{W} \sin\alpha_j$$ (Eq 6.29) 6.16

$$n_{z_{max}} = \frac{C_{L_{max}} q}{(W/S)_{min}}$$ (Eq 6.30) 6.17

$$n_{z_{max}} = \frac{C_{L_{max}}}{(W/S)_{min}} 0.7\; P_a M^2$$ (Eq 6.31) 6.17

$$n_{z_{max}} = K M^2$$ (Eq 6.32) 6.17

$$K = \frac{0.7}{(W/S)} C_{L_{max}} P_a$$ (Eq 6.33) 6.17

$$\frac{1}{V_{s\,(1g)}^{\;2}} = \frac{n_L}{V_A^{\;2}}$$ (Eq 6.34) 6.18

$$V_A = V_{s_{(1g)}} \sqrt{n_L}$$ (Eq 6.35) 6.18

$$R = \frac{a^2 M^2}{g\sqrt{K^2 M^4 - 1}}$$ (Eq 6.36) 6.20

$$\omega = \frac{g\sqrt{K^2 M^4 - 1}}{a M}$$ (Eq 6.37) 6.21

$$K = \frac{0.7}{(W/S)} C_{L_{max}} P_a$$ (Eq 6.38) 6.21

$$R_{min_{V>V_A}} = \left(\frac{a^2}{g\sqrt{n_L^2 - 1}}\right) M^2$$ (Eq 6.39) 6.23

$$\omega_{max_{V>V_A}} = \left(\frac{g\sqrt{n_L^2 - 1}}{a}\right) \frac{1}{M}$$ (Eq 6.40) 6.23

$$D = \frac{C_D}{C_L} L$$ (Eq 6.41) 6.29

$$T = \frac{C_D}{C_L} n_z W$$ (Eq 6.42) 6.29

$$n_z = \frac{T}{W} \frac{C_L}{C_D}$$ (Eq 6.43) 6.29

$$n_{z_{sust_{max}}} = \frac{T}{W} \left(\frac{C_L}{C_D}\right)_{max} \quad \text{(Jet)}$$ (Eq 6.44) 6.29

$$n_z = \frac{T(V_T)}{W} \frac{L}{D(V_T)}$$ (Eq 6.45) 6.29

$$n_{z_{sust_{max}}} = \frac{THP_{avail}}{W} \frac{L}{(THP_{req})_{min}} \quad \text{(Propeller)}$$ (Eq 6.46) 6.30

$$\omega_{sust} = \frac{57.3\, g}{V_T} \sqrt{n_{z_{sust}}^2 - 1} \quad \text{(deg/s)}$$ (Eq 6.47) 6.30

$$R_{sust} = \frac{V_T^{\,2}}{g\sqrt{n_{z_{sust}}^2 - 1}}$$ (Eq 6.48) 6.30

$$\frac{T}{\delta} = f\left(M, \frac{\dot{W}_f}{\delta_T \sqrt{\theta_T}}\right)$$ (Eq 6.49) 6.32

$$\frac{\Delta D}{\delta} = \frac{\Delta T}{\delta}$$ (Eq 6.50) 6.33

$$\Delta D_{Std\text{-}Test} = \frac{1}{\pi e AR\ S\ (0.7)\ P_{ssl}\ \delta_{Test}\ M^2}\left[\left(n_z W\right)^2_{Std} - \left(n_z W\right)^2_{Test}\right]$$ (Eq 6.51) 6.34

$$n_{z_{Std}} = \sqrt{\frac{1}{W^2_{Std}}\left[\left(n_z W\right)^2_{Test} + \Delta T\ \pi\ e\ AR\ (0.7)\ S\ P_{ssl}\ \delta_{Test}\ M^2\right]}$$ (Eq 6.52) 6.34

$$n_{z_{Std}} = n_{z_{Test}}\left(\frac{W_{Test}}{W_{Std}}\right)$$ (Eq 6.53) 6.35

$$T_{ex} = T - D = \frac{W}{V_T}\frac{dh}{dt} + \frac{W}{g}\frac{dV_T}{dt}$$ (Eq 6.54) 6.38

$$\frac{dV_T}{dt} = \frac{11.3\ \ P_s}{V_T}$$ (Eq 6.55) 6.48

$$n_z = n_{z_o} + \Delta n_{ic} + \Delta n_{z\ tare}$$ (Eq 6.56) 6.57

$$V_i = V_o + \Delta V_{ic}$$ (Eq 6.57) 6.63

$$V_c = V_i + \Delta V_{pos}$$ (Eq 6.58) 6.63

$$H_{P_i} = H_{P_o} + \Delta H_{P_{ic}}$$ (Eq 6.59) 6.63

$$H_{P_c} = H_{P_i} + \Delta H_{pos}$$ (Eq 6.60) 6.63

$$n_{z_i} = n_{z_o} + \Delta n_{z_{ic}}$$ (Eq 6.61) 6.63

$$n_{z_{Test}} = n_{z_i} + \Delta n_{z_{tare}}$$ (Eq 6.62) 6.63

$$C_{L_{max_{Test}}} = \frac{n_{z_{Test}} W_{Test}}{0.7\, P_{ssl}\, \delta_{Test}\, M^2\, S}$$ (Eq 6.63) 6.63

$$V_T = a\, M$$ (Eq 6.64) 6.64

$$\Delta T = T_{Std} - T$$ (Eq 6.65) 6.66

$$n_{z_{sust}} = \sqrt{\frac{P_{s_{1g}}\, \pi\, e\, AR\, S\;\, 0.7\, P_{ssl} \delta\, M^2}{V_T W_{Std}} + 1}$$ (Eq 6.66) 6.68

$$T_{ex} = T - D = \frac{W_{Std}}{V_T}\, P_{s_{1g}}$$ (Eq 6.67) 6.68

$$n_{z_{sust}} = \sqrt{\left(\frac{n_z W_{Std}}{\delta M}\right)^2 \frac{\delta_h}{W_{Std}}\, M}$$ (Eq 6.68) 6.68

$$n_z = \left(\frac{\delta}{W}\right)\left(0.7\, P_{ssl}\, S\right) C_L\, M^2$$ (Eq 6.69) 6.71

$$\left(n_z \frac{W}{\delta}\right)_{Test} = \left(0.7\, P_{ssl}\, S\right) C_L\, M^2$$ (Eq 6.70) 6.71

CHAPTER 6

TURN PERFORMANCE AND AGILITY

6.1 INTRODUCTION

This chapter covers airplane turning performance and agility characteristics. Sustained and instantaneous turn performance characteristics are developed, and measures of agility are presented. Test techniques are described for documenting turn rate, turn radius, and excess energy while maneuvering. Data reduction methods and analysis techniques are described for evaluating and comparing airplane turning performance and maneuvering characteristics.

6.2 PURPOSE OF TEST

The purpose of these tests is to determine the turning performance and maneuvering characteristics of the airplane, with the following objectives:

1. Measure sustained and instantaneous turn performance.
2. Measure maneuvering excess energy characteristics.
3. Present agility measures and airplane comparison methods.
4. Define mission suitability issues.

6.3 THEORY

6.3.1 MANEUVERING

An airplane inflight has a velocity vector which defines its speed and direction of flight. The capacity to change this vector is called maneuverability. Quantifying the maneuverability of an airplane involves documenting the acceleration, deceleration, and turning characteristics. These characteristics are not independent, as the analysis shows; however, they can be isolated for study with the help of specialized test techniques. The level acceleration testing, introduced in Chapter 5, isolated the acceleration characteristics from the increased drag of turning flight. In this chapter, turn performance is introduced at constant speed, to isolate the turning characteristics from flight path accelerations. Then, the combined characteristics of accelerations and turns are addressed using a total energy approach.

In maneuvering, the forces of lift, weight, thrust, and drag are altered to generate linear or radial accelerations. The radial acceleration causes a turn in the horizontal, in the vertical, or in an oblique plane. Forces which cause a radial acceleration include: weight, sideforce, lift, and thrust (although thrust is easily included in the lift and sideforce terms). Each of these forces can curve the flight path, turning the airplane. Visualizing how weight can turn the flight path is easy. For example, at zero g (though the resulting ballistic flight path is not generally thought of as a turn). Sideforce can cause the flight path to curve, allowing level turns to be performed at zero bank angle. The most common force used to turn, however, is the lift force. Lift variations at zero bank angle can cause the flight path to curve up or down, but most turns are performed by tilting the lift vector from the vertical. Generally, a turn has vertical and horizontal components, although the one easiest to analyze is the level turn.

6.3.2 LEVEL TURNS

All of the forces which can be used to alter the velocity vector contribute to maneuverability. For level turns the turning forces are lift, thrust, and sideforce. Lift is the primary force and is investigated first. Turn radius and turn rate expressions are developed, then the effects of sideforce and thrust are discussed.

6.3.2.1 FORCES IN A TURN

Consider an airplane in a steady, level turn which is coordinated in the sense sideforce is zero, as depicted in figure 6.1.

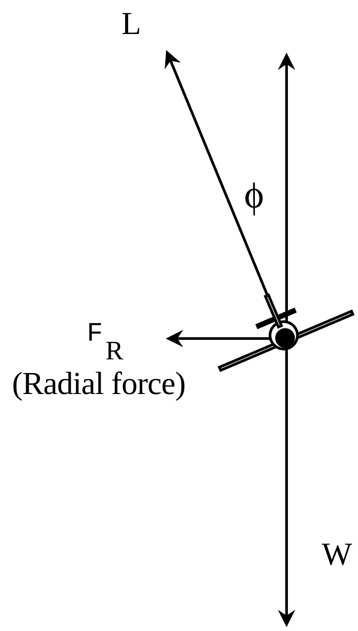

Figure 6.1
FORCES IN A STEADY LEVEL TURN

The turning force produces a radial acceleration which can be measured. The following steps derive an expression for the radial acceleration. Load factor, n_z, is defined by the expression:

$$n_z = \frac{L}{W} \tag{Eq 6.1}$$

From the right triangle of lift and its components:

$$L^2 = W^2 + (W \tan \phi)^2 \tag{Eq 6.2}$$

Dividing by W^2, gives:

$$n_z^2 = 1 + \tan^2 \phi \tag{Eq 6.3}$$

Or:

$$\tan \phi = \sqrt{\left(n_z^2 - 1\right)} \quad \text{(Eq 6.4)}$$

Summing the forces in the vertical yields:

$$L \cos \phi = W \quad \text{(Eq 6.5)}$$

Substituting for W using Eq 6.1:

$$n_z = \frac{1}{\cos \phi} \quad \text{(Eq 6.6)}$$

The horizontal summation yields:

$$W \tan \phi = \frac{W}{g} a_R \quad \text{(Eq 6.7)}$$

Simplifying, and rearranging gives an expression for a_R:

$$a_R = g \tan \phi \quad \text{(Eq 6.8)}$$

In terms of load factor:

$$a_R = g \sqrt{\left(n_z^2 - 1\right)} \quad \text{(Eq 6.9)}$$

Where:

a_R	Radial acceleration	ft/s^2
ϕ	Bank angle	deg
g	Gravitational acceleration	ft/s^2
L	Lift	lb
n_z	Normal acceleration	g
W	Weight	lb.

6.3.2.2 TURN RADIUS AND TURN RATE

The primary characteristics which describe a turn are the turn radius and turn rate. Expressions for these characteristics are developed using the following depiction of an airplane in a steady, level turn (Figure 6.2).

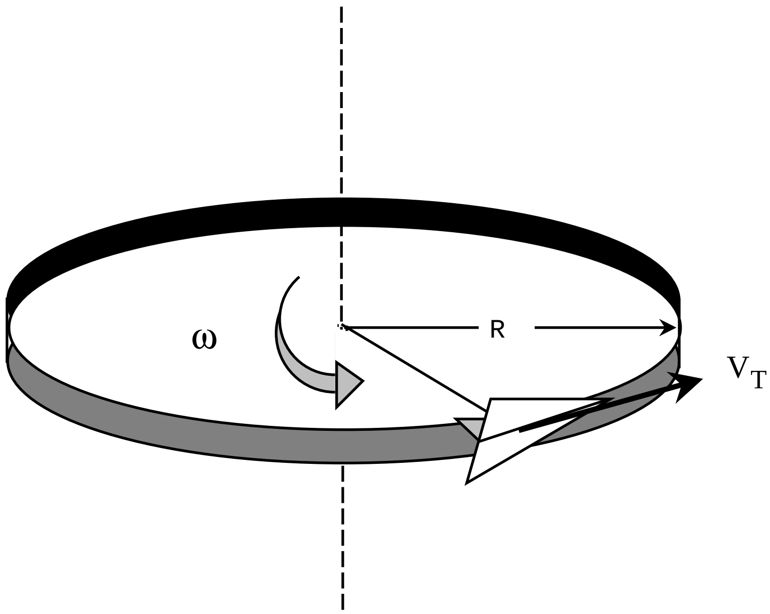

Figure 6.2
STEADY TURN DIAGRAM

The radius, R, of a level turn is calculated using the following relationship:

$$R = \frac{V_T^2}{a_R} \qquad \text{(Eq 6.10)}$$

Substituting for a_R, using Eq 6.8:

$$R = \frac{V_T^2}{g \tan \phi} \qquad \text{(Eq 6.11)}$$

Using Eq 6.9:

$$R = \frac{V_T^2}{g\sqrt{\left(n_z^2 - 1\right)}} \qquad \text{(Eq 6.12)}$$

Turn radius varies with true airspeed and load factor as depicted in figure 6.3.

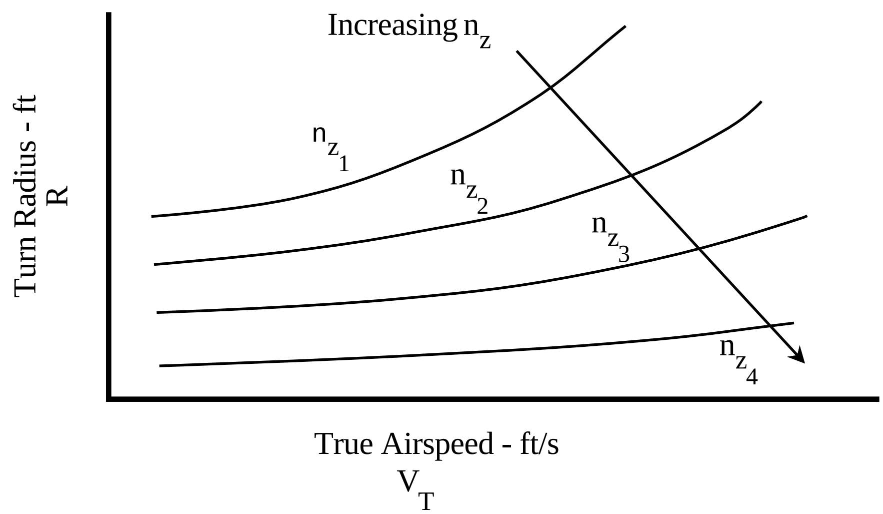

Figure 6.3
TURN RADIUS

Turn rate, ω, is expressed as:

$$\omega = \frac{V_T}{R} \qquad \text{(Eq 6.13)}$$

Eq 6.11 or 6.12 can be used to calculate turn rate as follows:

$$\omega = \frac{g}{V_T} \tan \phi \qquad \text{(Eq 6.14)}$$

$$\omega = \frac{g}{V_T} \sqrt{\left(n_z^2 - 1\right)} \qquad \text{(Eq 6.15)}$$

Where:

a_R	Radial acceleration	ft/s^2
ϕ	Bank angle	deg
g	Gravitational acceleration	ft/s^2
n_z	Normal acceleration	g
R	Turn radius	ft
V_T	True airspeed	ft/s
ω	Turn rate	rad/s.

Turn rate varies with true airspeed and load factor as depicted in figure 6.4. A line, from the origin, representing a constant $\frac{\omega}{V_T}$, relates to a particular turn radius.

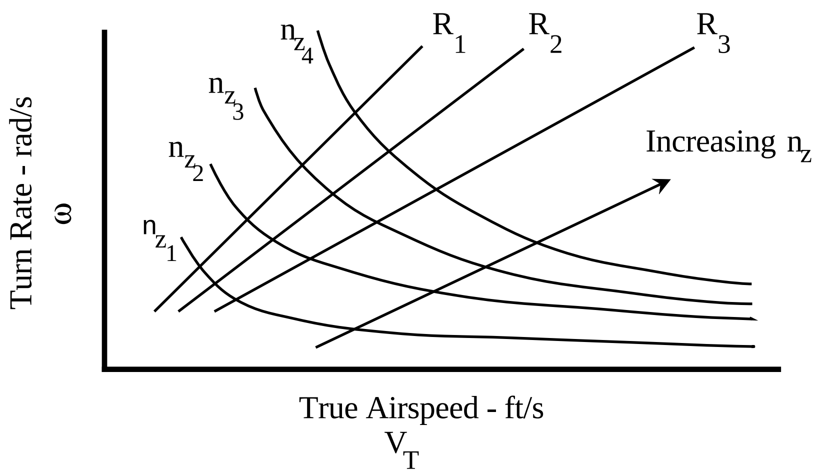

Figure 6.4
TURN RATE

6.3.2.3 SIDEFORCE EFFECTS

The preceding treatment of level turns dealt exclusively with coordinated turns, turns with no sideforce. To see the effects of non-zero sideforce, consider an airplane in a wings-level steady turn, as shown in figure 6.5(a).

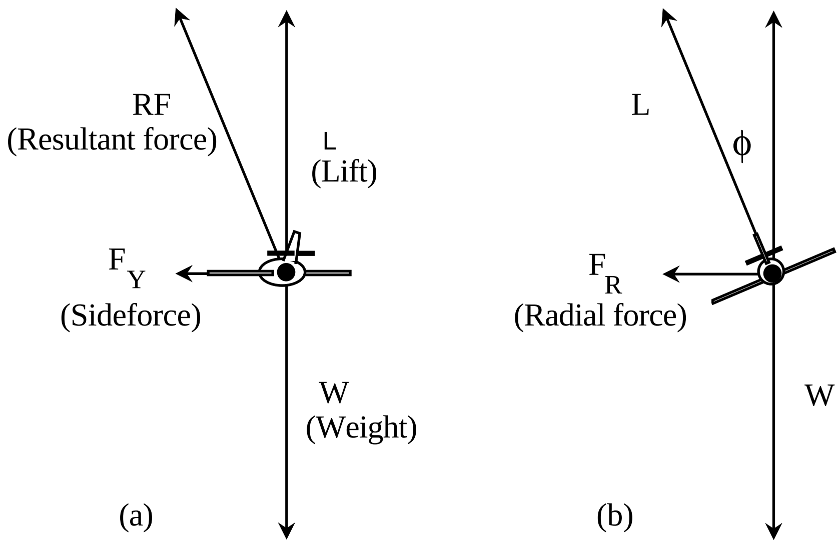

Figure 6.5

FLAT TURN AND COORDINATED TURN COMPARISON

For this example, the sideforce, F_Y, is a purely radial force which produces a flat turn (zero bank angle). An equivalent coordinated turn, shown in figure 6.5(b), results if the airplane is banked to an angle, ϕ:

$$\phi = \tan^{-1}\left(\frac{F_Y}{W}\right) \quad \text{(Eq 6.16)}$$

The lift, L, required in this case is:

$$L = \frac{W}{\cos \phi} \quad \text{(Eq 6.17)}$$

Next, consider the effect of sideforce in a steady uncoordinated turn, as shown in figure 6.6.

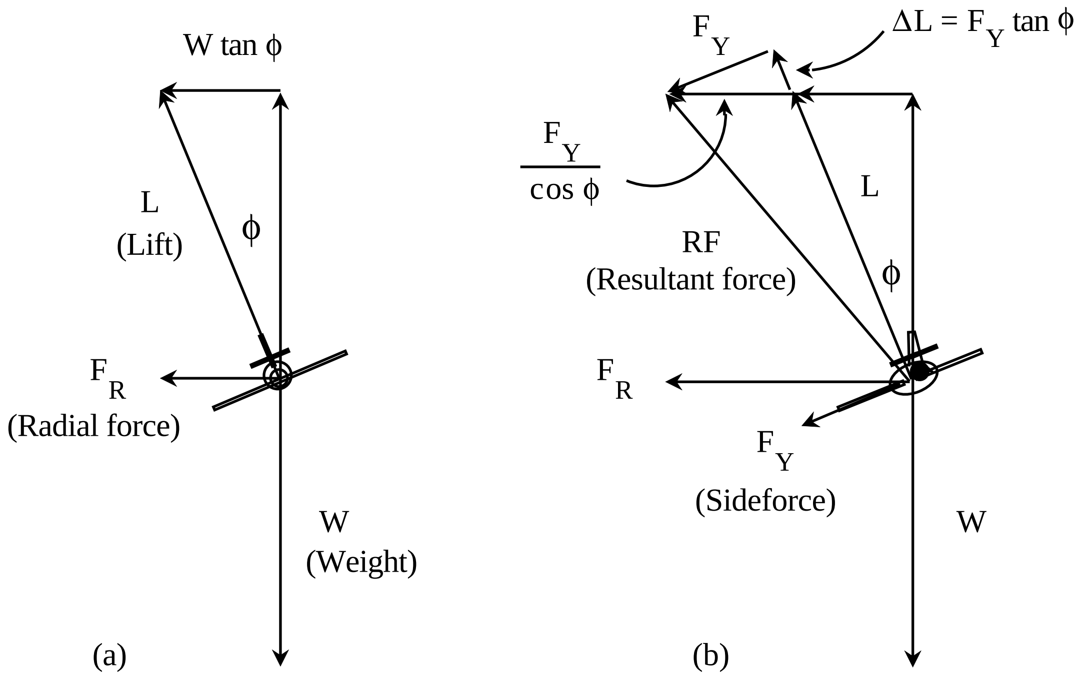

Figure 6.6

COORDINATED AND UNCOORDINATED TURN COMPARISON

Figure 6.6 (a) depicts the airplane in a steady turn of constant bank angle ϕ, with no sideforce. In this case, the resultant force and the lift are the same, and equal to $\frac{W}{\cos\phi}$. Figure 6.6 (b) shows the addition of sideforce in the direction of the turn, keeping the bank angle constant. Notice that the resultant force is no longer coincident with the lift, but its vertical component must remain equal to W. An increase in lift, ΔL, is required (at some drag penalty) to offset the negative lift from the sideforce. This extra lift requirement depends upon the amount of sideforce and the angle of bank, according to the expression:

$$\Delta L = F_Y \tan\phi \qquad \text{(Eq 6.18)}$$

The radial force for this example is greater than for figure 6.6 (a) by the increment $\frac{F_Y}{\cos\phi}$, composed of the radial components of F_Y and ΔL. The total radial force is expressed as:

$$F_R = W \tan\phi + \frac{F_Y}{\cos\phi} \qquad \text{(Eq 6.19)}$$

Normalizing, to get load factor terms:

$$n_R = \tan\phi + \frac{n_Y}{\cos\phi} \qquad \text{(Eq 6.20)}$$

The resulting turn is equivalent to a coordinated turn at the equivalent bank angle, ϕ_E, as shown below:

$$\phi_E = \tan^{-1}\left(\tan\phi + \frac{n_Y}{\cos\phi}\right) \qquad \text{(Eq 6.21)}$$

Expressions for turn radius and turn rate which include a sideforce term are:

$$R = \frac{V_T^2}{g\left(\tan\phi + \frac{n_Y}{\cos\phi}\right)} \qquad \text{(Eq 6.22)}$$

And:

$$\omega = \frac{g\left(\tan\phi + \frac{n_Y}{\cos\phi}\right)}{V_T} \qquad \text{(Eq 6.23)}$$

Note if $n_Y = 0$, the above equations reduce to the form of Eq 6.11 and 6.14, for coordinated turns.

The presence of sideforce in a turn alters the turn rate and radius. The increase in turn rate with augmenting sideforce, $\Delta\omega$, is expressed by:

$$\Delta\omega = \frac{g\, n_Y}{V_T \cos\phi} \qquad \text{(Eq 6.24)}$$

Where:

ϕ	Bank angle	deg
ϕ_E	Equivalent bank angle	deg
F_R	Radial force	lb
F_Y	Sideforce	lb
g	Gravitational acceleration	ft/s^2
n_R	Radial load factor, $\frac{F_R}{W}$	g
n_Y	Sideforce load factor, $\frac{F_Y}{W}$	g
n_z	Normal acceleration	g
R	Turn radius	ft
V_T	True airspeed	ft/s
ω	Turn rate	rad/s.

Though it appears sideforce can be used to augment turning performance, in practice it is a relatively inefficient and uncomfortable means to turn. It may have potential uses, however, in decoupled control modes of fly-by-wire airplanes. For example, direct sideforce control can be used to turn without banking for course corrections in a weapons delivery mode.

6.3.2.4 THRUST EFFECTS

For this discussion, the thrust component of lift is assumed constant and is absorbed in the lift term. In practice, the thrust component may be significant if thrust lift is a large percentage of total lift. Later sections present the effects of thrust lift, particularly low speed effects with vectored thrust.

6.3.3 VERTICAL TURNS

Vertical turns highlight the influence of the weight vector on turns. In the level turn, weight does not contribute to the radial force. In the vertical turn, however, weight contributes directly to the radial force. The contribution depends upon the changing orientation of the lift and weight vectors in the vertical turn. Consider the variation of radial acceleration for a constant speed loop, with a constant 4 g indicated on the cockpit accelerometer, as shown in figure 6.7.

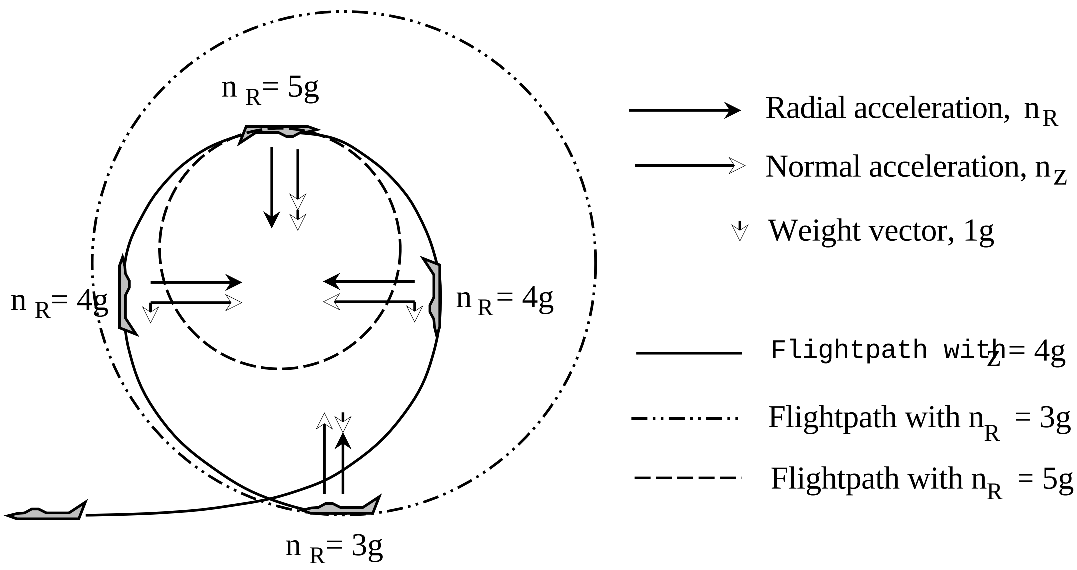

Figure 6.7

VARIATION OF RADIAL ACCELERATION IN A CONSTANT SPEED, 4 G LOOP

The radial load factor can be expressed as:

$$n_R = n_z - \cos\gamma \quad \text{(Eq 6.25)}$$

The changing radial acceleration causes the turn radius and turn rate to vary, as well. The generalized expressions for turn radius and turn rate are:

$$R_{(\text{wings level})} = \frac{V_T^2}{g\,(n_z - \cos\gamma)} \quad \text{(Eq 6.26)}$$

and,

$$\omega_{(\text{wings level})} = \frac{g\,(n_z - \cos\gamma)}{V_T} \quad \text{(Eq 6.27)}$$

Where:

γ	Flight path angle	deg
g	Gravitational acceleration	ft/s^2
n_R	Radial load factor	g
n_z	Normal acceleration	g
R	Turn radius	ft
V_T	True airspeed	ft/s
ω	Turn rate	rad/s.

The orientation of the lift vector to the weight vector has a significant effect on turn performance, as shown in the following turn data from 15,000 ft. Figure 6.8 presents the turning capability of an airplane in different orientations. In this figure, the typical horizontal turn is compared to turns in the vertical plane. The pull-up and pull-down cases are similar to the bottom and the top of a loop, respectively. The straight up/down data refer to the cases where the pitch attitude is plus or minus 90 deg.

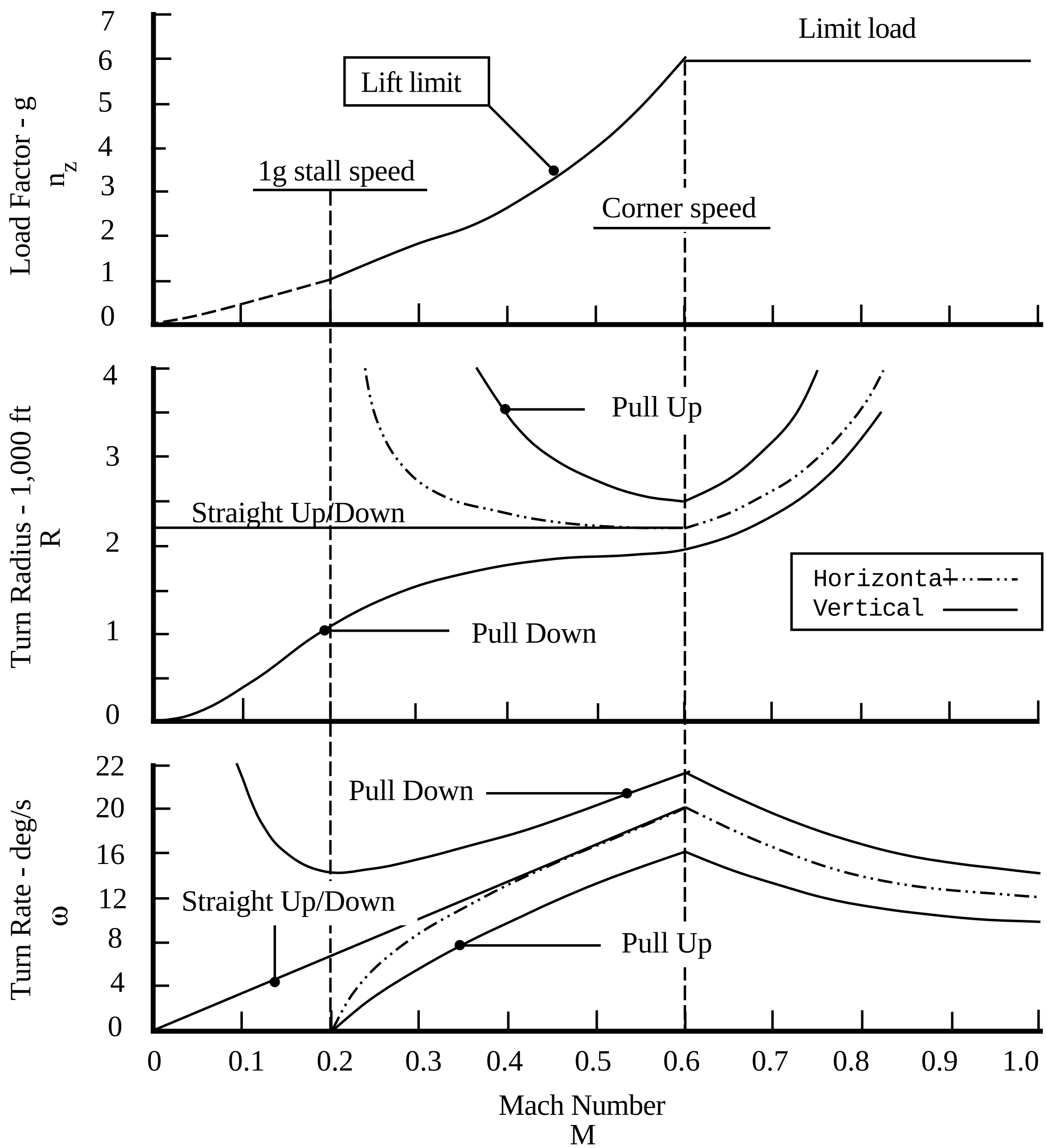

Figure 6.8
VERTICAL TURN PERFORMANCE

The weight vector can be used to tighten a turn, only if the lift vector is pointed below the horizon. Whenever the nose of the airplane is pulled up, the turn is hampered by the weight vector. The advantage of using the weight vector to tighten a turn is short-lived, but it can be exploited in a variety of tactical situations.

6.3.4 INSTANTANEOUS TURN PERFORMANCE

Instantaneous performance describes the capability of an airplane at a particular flight condition, at an instant in time. There is no consideration of the airplane's ability to sustain the performance for any length of time, nor is there any consideration of the energy rate at these conditions. Energy loss rate may be high, and is manifested usually by rapid deceleration or altitude loss. The engine is capable of changing the energy loss rate at these conditions. The energy situation is covered in a later section. First, consider the maneuvering potential of the airframe alone. Instantaneous turn performance is a function of the lift capability and the structural strength of the airframe.

6.3.4.1 THE V-N DIAGRAM

The V-n diagram is a useful format for presenting airframe lift capabilities and structural strength limitations. On this plot, airplane operating envelopes are mapped on a grid of airspeed and load factor. Any set of criteria can be used to define envelope boundaries on a V-n diagram. For example, the operational, service, and permissible envelopes referred to in the fixed wing flying qualities specification are described by V-n diagrams. However, the most common V-n diagram describes maximum aerodynamic capabilities and strength limitations, as depicted in figure 6.9.

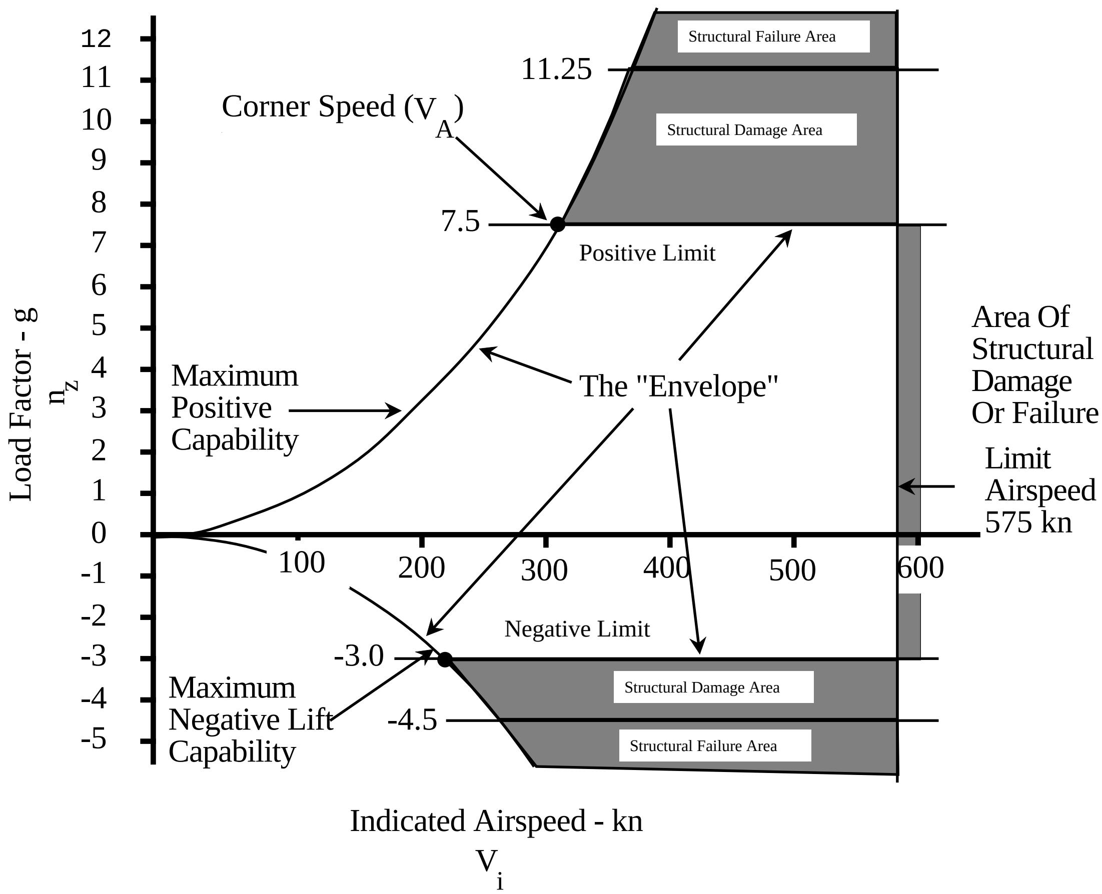

Figure 6.9
THE V-N DIAGRAM

Beginning at zero airspeed, two curves diverge to describe the maximum lift boundaries for positive and negative load factors. Since the lines represent stall, operations to the left of these curves are beyond the capability of the airplane, except in dynamic, unsteady maneuvers such as zoom climbs. From the example shown, steady flight is not attainable below 100 kn, the 1 g stall speed. At 200 kn, 4 g is attainable, and so on, with increasing load factor capability as speed is increased. At some speed, the load factor available is equal to the load limit of the airframe, n_L. This speed is called the corner speed or maneuvering speed, $V_{A.}$ The significance of V_A is developed in later sections. The same constraints define the negative load factor capabilities and negative g corner speed. Notice the negative g available at any particular speed is typically lower than the positive g available, due to the wing camber and control power effects. The envelope is bounded on the right for all load factors by the limit airspeed, V_L.

The lift boundary of the V-n diagram is the primary focus of flight test documentation. The airplane is able to develop n_L at all speeds above V_A, though it may be difficult to verify near V_L due to the deceleration experienced while pulling to n_L. For airspeeds above V_A, calculations of instantaneous turn performance parameters can be made without documentation, based on the constant n_L out to V_L. Flight tests are required, however, to document the boundary imposed by the lift limit, where the maximum load factor is diminished. The measure of instantaneous maneuverability is not only a high n_L, but also a low V_A.

6.3.4.2 LIFT LIMIT

The emphasis in this section is on the limitation to instantaneous turn performance imposed by the airplane lift capability. The forces contributing to lift are shown in figure 6.10.

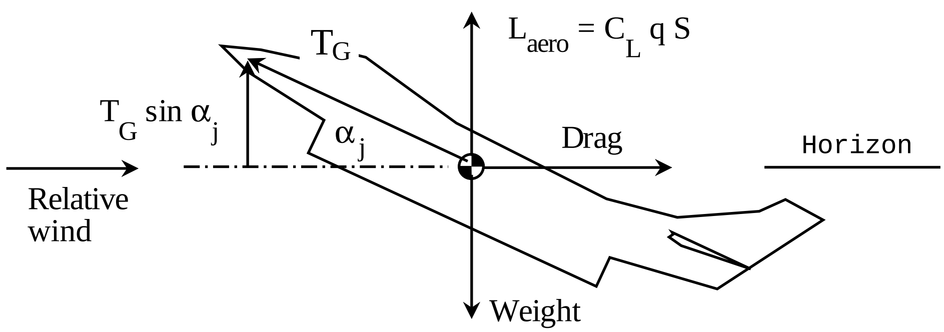

Figure 6.10
FORCES CONTRIBUTING TO LIFT

Total lift is expressed as the sum of aerodynamic lift and thrust lift.

$$L = C_L q\, S + T_G \sin \alpha_j \qquad \text{(Eq 6.28)}$$

Normalizing, by dividing by weight,W:

$$n_z = \frac{C_L q}{W/S} + \frac{T_G}{W} \sin \alpha_j \qquad \text{(Eq 6.29)}$$

Neglecting thrust effects, the load factor is a function of lift coefficient, dynamic pressure, and wing loading. For a given set of test conditions (altitude and Mach number), the maximum load factor is attained when C_L is maximum and W/S is a minimum:

$$n_{z_{max}} = \frac{C_{L_{max}} q}{(W/S)_{min}} \quad \text{(Eq 6.30)}$$

Instantaneous turn performance demands high $C_{L_{max}}$ and low wing loading for attaining high load factors. The maximum lift coefficient is limited by aerodynamic stall, maximum control deflection, or any of a number of adverse flying qualities (see Chapter 3 for additional discussion of stall). Wing loading is variable, since gross weight decreases with fuel depletion and the release of external stores. On some airplanes, variable wing sweep can change the effective wing surface area.

Expressing dynamic pressure in terms of Mach number gives:

$$n_{z_{max}} = \frac{C_{L_{max}}}{(W/S)_{min}} \; 0.7 \; P_a M^2 \quad \text{(Eq 6.31)}$$

Regrouping:

$$n_{z_{max}} = K M^2 \quad \text{(Eq 6.32)}$$

Where:

$$K = \frac{0.7}{(W/S)} C_{L_{max}} P_a \quad \text{(Eq 6.33)}$$

The following depicts the functional relationship:

$$n_{z_{max}} = f\left(C_{L_{max}}, \frac{W}{S}, H_p, M^2\right)$$

From Eq 6.32, the variation of $n_{z_{max}}$ with Mach number for a particular altitude is parabolic, if $C_{L_{max}}$ and W/S are constant, as shown in figure 6.11.

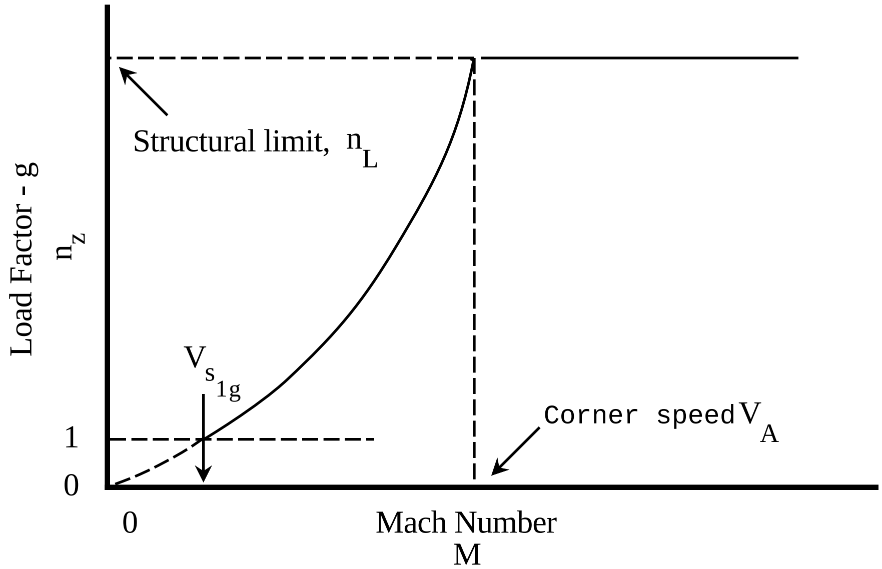

Figure 6.11
MAXIMUM INSTANTANEOUS LOAD FACTOR

This shape is characteristic for the lift boundary of the V-n diagram. If the 1 g stall speed is known, a simple calculation reveals the predicted corner speed, V_A. Since $\frac{n_{z_{max}}}{M^2}$ is constant along the curve, so is $\frac{n_{z_{max}}}{V^2}$. Thus:

$$\frac{1}{V_{s_{(1g)}}^2} = \frac{n_L}{V_A^2} \tag{Eq 6.34}$$

And,

$$V_A = V_{s_{(1g)}} \sqrt{n_L} \tag{Eq 6.35}$$

Where:

α_j	Thrust angle	deg
C_L	Lift coefficient	
$C_{L_{max}}$	Maximum lift coefficient	
H_P	Pressure altitude	ft
K	Constant	
L	Lift	lb
L_{aero}	Aerodynamic lift	lb

M	Mach number	
n_L	Limit normal acceleration	g
n_z	Normal acceleration	g
$n_{z_{max}}$	Maximum normal acceleration	g
P_a	Ambient pressure	psf
q	Dynamic pressure	psf
S	Wing area	ft^2
T_G	Gross thrust	lb
V_A	Maneuvering speed	kn, ft/s
V_s	Stall speed	kn or ft/s
W	Weight	lb.

In arriving at figure 6.11, a constant $C_{L_{max}}$ is assumed. This assumption is valid at low Mach number. At higher Mach number compressibility effects must be considered.

6.3.4.3 VARIATION OF MAXIMUM LIFT COEFFICIENT WITH MACH NUMBER

The typical variation of $C_{L_{max}}$ with Mach number for a constant altitude is depicted in figure 6.12.

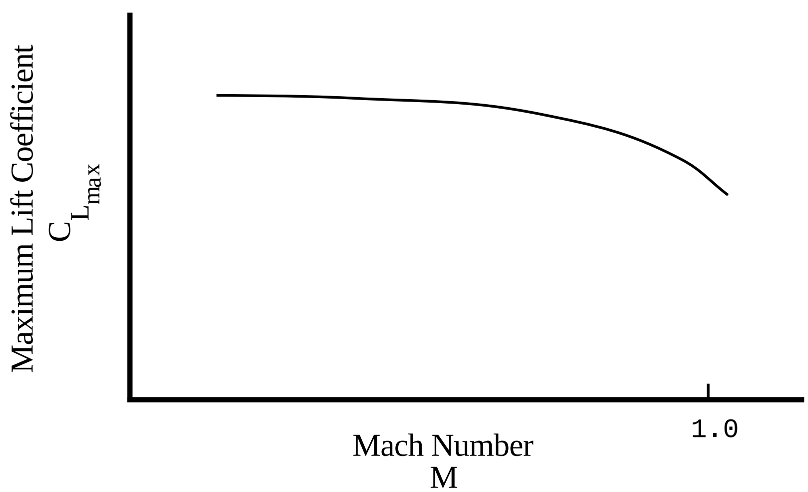

Figure 6.12
VARIATION OF MAXIMUM LIFT COEFFICIENT WITH MACH NUMBER

Up to about 0.7 Mach number, $C_{L_{max}}$ is essentially constant, even for a wing with a relatively thick airfoil section. At higher Mach number, a transonic reduction in $C_{L_{max}}$ is noted, which may begin below the corner speed. The expected reduction in $n_{z_{max}}$ is illustrated in figure 6.13.

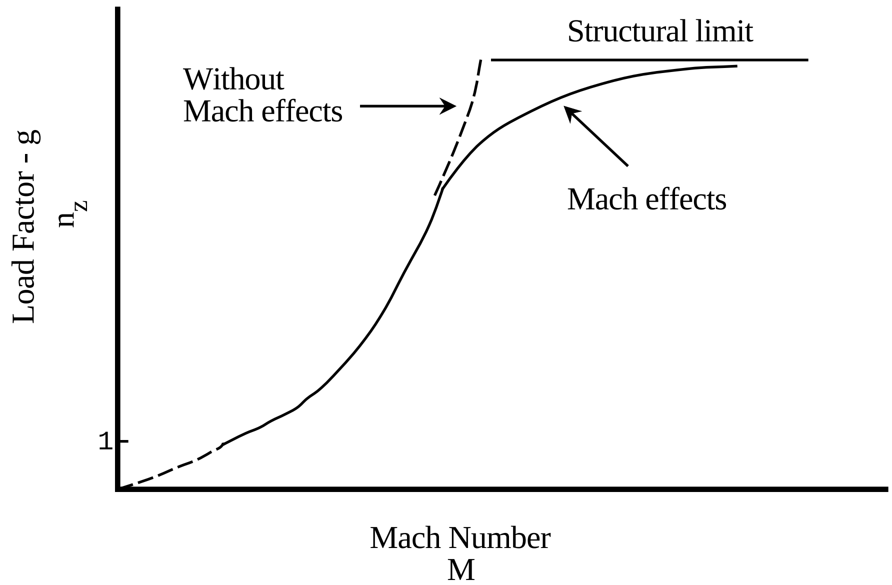

Figure 6.13
MAXIMUM INSTANTANEOUS LOAD FACTOR WITH COMPRESSIBILITY EFFECTS

High performance airplanes, particularly supersonic interceptors and fighters, exhibit this characteristic Mach number effect.

6.3.4.4 INSTANTANEOUS TURN RADIUS AND RATE

Instantaneous turn radius and turn rate vary with Mach number according to these relationships derived from Eq 6.12 and 6.15:

$$R = \frac{a^2 M^2}{g \sqrt{K^2 M^4 - 1}} \qquad \text{(Eq 6.36)}$$

And:

$$\omega = \frac{g\sqrt{K^2 M^4 - 1}}{a M} \qquad \text{(Eq 6.37)}$$

Where:

$$K = \frac{0.7}{(W/S)} C_{L_{max}} P_a \qquad \text{(Eq 6.38)}$$

Where:

a	Speed of sound	ft/s
$C_{L_{max}}$	Maximum lift coefficient	
g	Gravitational acceleration	ft/s^2
K	Constant	
M	Mach number	
P_a	Ambient pressure	psf
R	Turn radius	ft
S	Wing area	ft^2
ω	Turn rate	rad/s
W	Weight	lb.

For a range of speeds where $C_{L_{max}}$ is constant at a particular altitude, K is constant. Figure 6.14 depicts instantaneous turn performance with constant K.

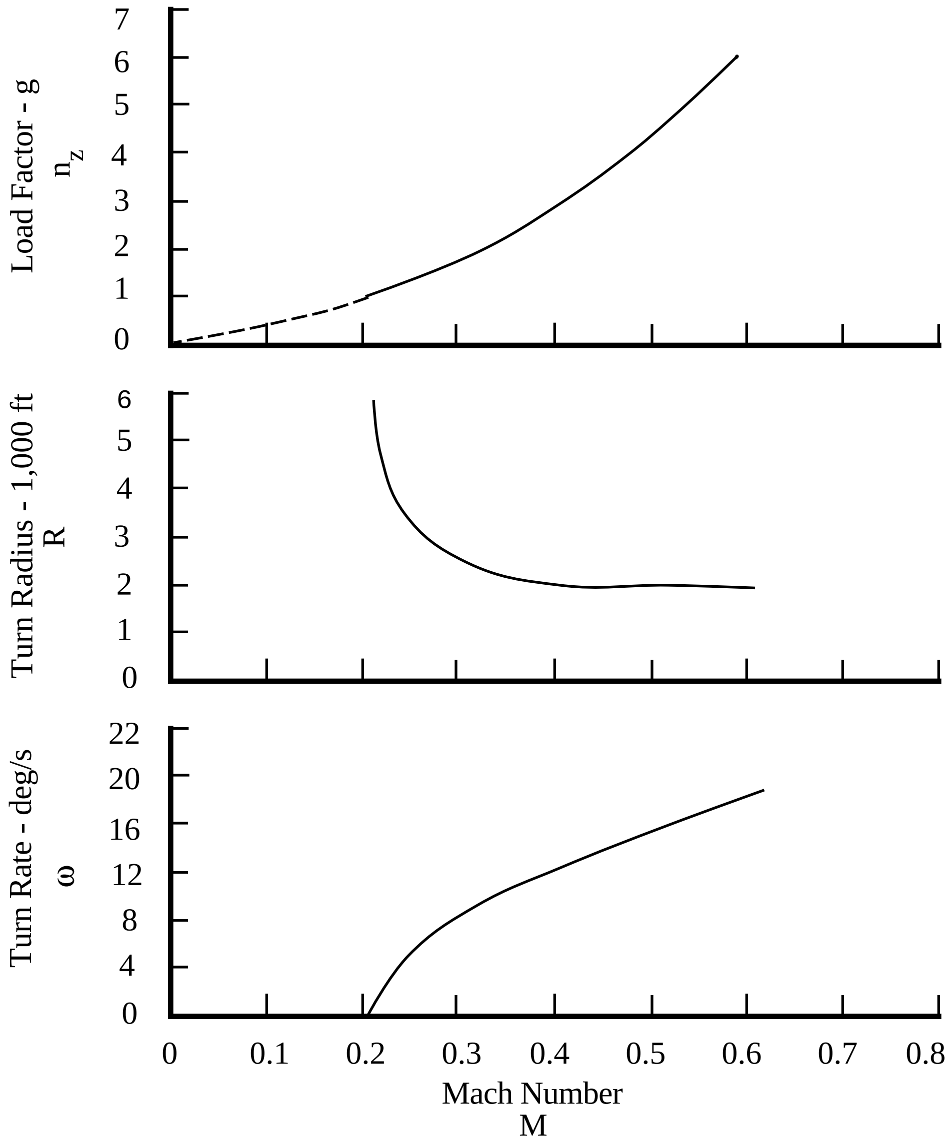

Figure 6.14
INSTANTANEOUS TURN PERFORMANCE USING CONSTANT MAXIMUM LIFT COEFFICIENT

At the 1 g stall speed, no turns can be made; turn radius is infinite and turn rate is zero. As airspeed is increased from the stall speed, turn radius rapidly diminishes, approaching a minimum at a relatively slow airspeed. Turn rate, on the other hand, continues to improve as speed is increased from the stall speed. Both curves become discontinuous at the corner speed, where the limit load factor forces a reduction in $C_{L_{max}}$ as speed increases (K is no longer constant).

6.3.4.5 STRUCTURAL LIMIT

Instantaneous turn performance improves with speed as long as load factor is allowed to increase. Beyond the corner speed, however, load factor is limited by structural strength. The decreases in instantaneous turn performance which result when load factor is limited are evident when examining the following relationships:

$$R_{min\ V>V_A} = \left(\frac{a^2}{g\sqrt{n_L^2 - 1}} \right) M^2 \qquad \text{(Eq 6.39)}$$

And,

$$\omega_{max\ V>V_A} = \left(\frac{g\sqrt{n_L^2 - 1}}{a} \right) \frac{1}{M} \qquad \text{(Eq 6.40)}$$

Where:

a	Speed of sound	ft/s
g	Gravitational acceleration	ft/s^2
M	Mach number	
n_L	Limit normal acceleration	g
$R_{min\ V>V_A}$	Minimum turn radius for $V > V_A$	ft
V_A	Maneuvering speed	ft/s
$\omega_{max\ V>V_A}$	Maximum turn rate for $V > V_A$	rad/s.

Since the quantities within the parentheses are constants, Eq 6.39 is a parabola, and Eq 6.40 is a hyperbola. Adding the segments representing the characteristics at speeds above V_A to figure 6.14, the following composite instantaneous turn performance graphs result (Figure 6.15).

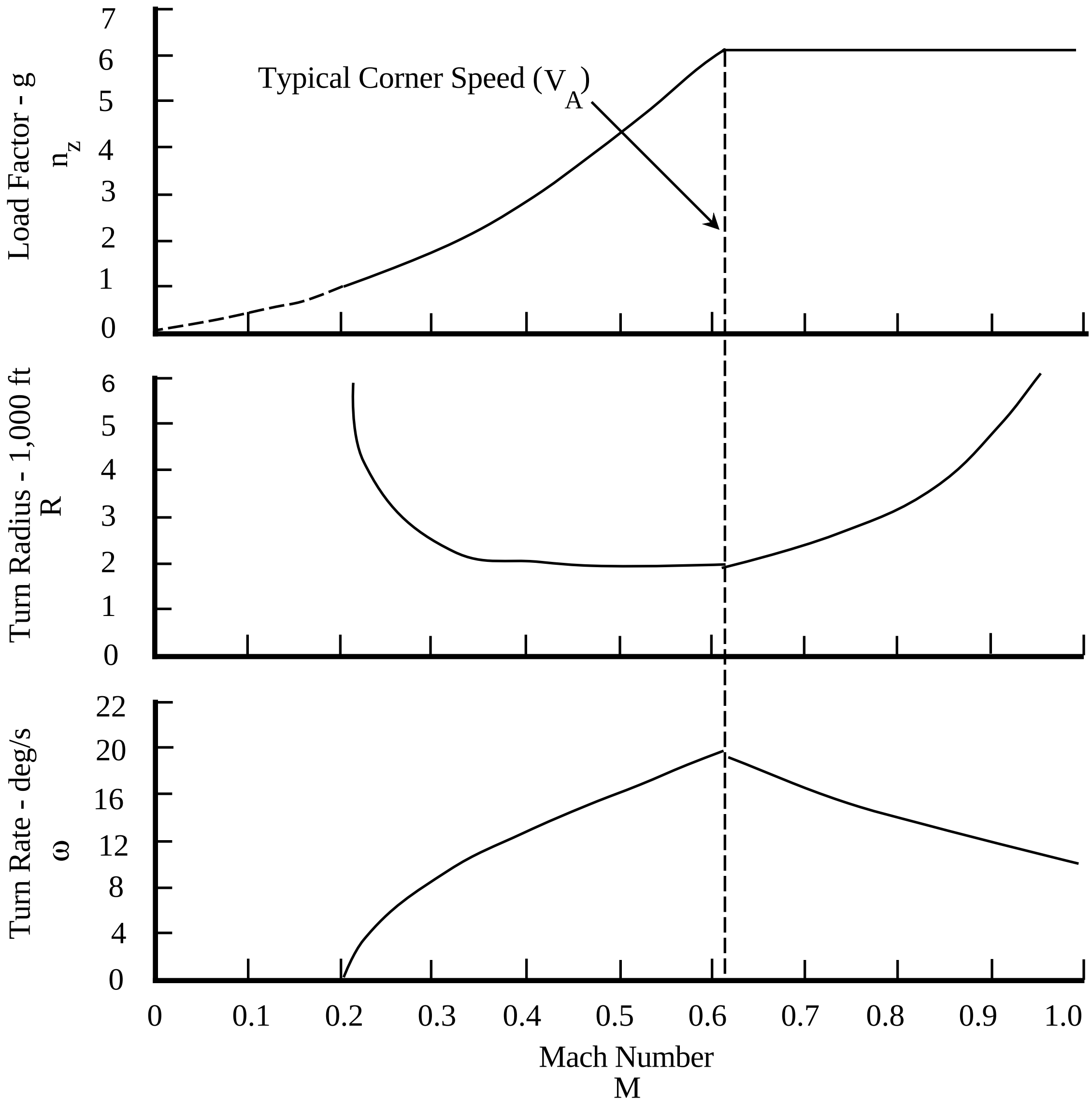

Figure 6.15

INSTANTANEOUS TURN PERFORMANCE

6.3.4.6 CORNER SPEED

The significance of the corner speed can be seen in figure 6.15. At the speed corresponding to the intersection of the lift boundary and the structural limit, the minimum instantaneous turn radius and maximum instantaneous turn rate are achieved. Thus, V_A is the speed for maximum turn performance when energy loss is not a consideration.

6.3.4.7 THRUST LIFT EFFECTS

In the previous discussions, thrust lift was neglected. Current technologies embracing high thrust-to-weight ratios and vectored thrust, however, make the thrust lift contribution significant. To investigate the effects of thrust lift on instantaneous turn performance, reexamine Eq 6.29, repeated here for convenience.

$$n_z = \frac{C_L q}{W/S} + \frac{T_G}{W} \sin \alpha_j \qquad \text{(Eq 6.29)}$$

Where:

α_j	Thrust angle	deg
C_L	Lift coefficient	
n_z	Normal acceleration	g
q	Dynamic pressure	psf
S	Wing area	ft^2
T_G	Gross thrust	lb
W	Weight	lb.

Considering an airplane with adjustable nozzles, like the Harrier, the thrust term in Eq 6.29 could approach unity. Thus, an incremental 1 g is provided by the thrust lift. The contribution from thrust lift is illustrated in figure 6.16, constructed by adding the incremental 1 g at all speeds to the curves in figure 6.15 (though still limited by n_L).

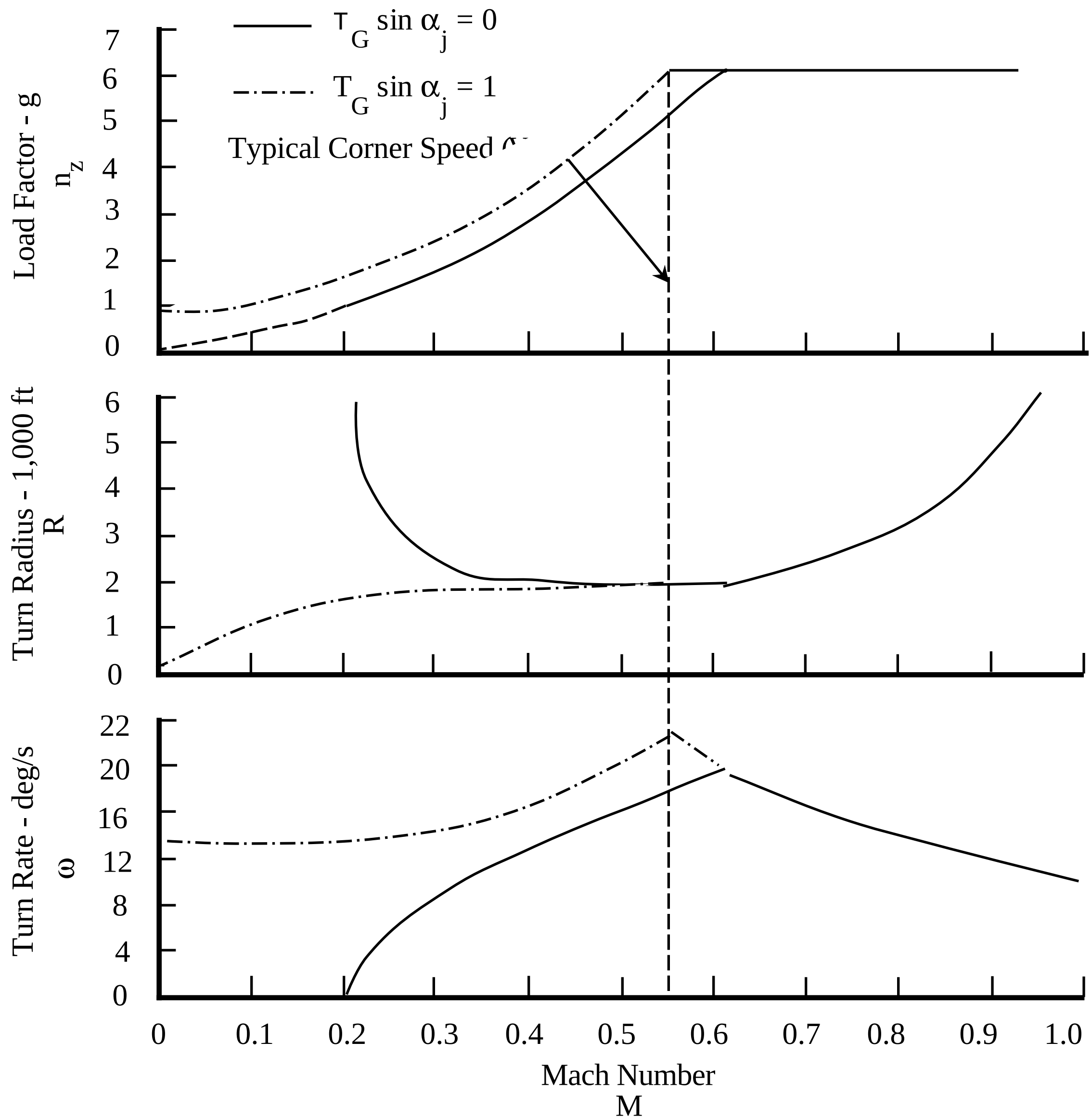

Figure 6.16
INSTANTANEOUS TURN PERFORMANCE WITH VECTORED THRUST

Significant improvements to instantaneous turn performance are realized at low airspeeds. At high airspeeds the vectored thrust contribution is small.

6.3.5 SUSTAINED TURN PERFORMANCE

The concept of sustained maneuverability is used to describe the airplane's ability to maneuver at constant altitude without losing energy and without decelerating. If the airplane is maintaining a level turn at constant airspeed and load factor, the forces along the flight path are balanced. Thrust equals drag for these conditions; therefore, the amount of maneuvering drag the airplane can balance is limited by the maximum thrust. Any changes in thrust available or drag will affect the sustained turning performance. The sustained turning capability may also be limited by airframe considerations.

For a level turn at a particular airspeed, the airplane uses excess thrust to counter the increased drag. Thrust available varies with ambient temperature, Mach number and altitude. Thrust required varies with Mach number and W/δ. Figure 6.17 depicts the difference between thrust available and thrust required.

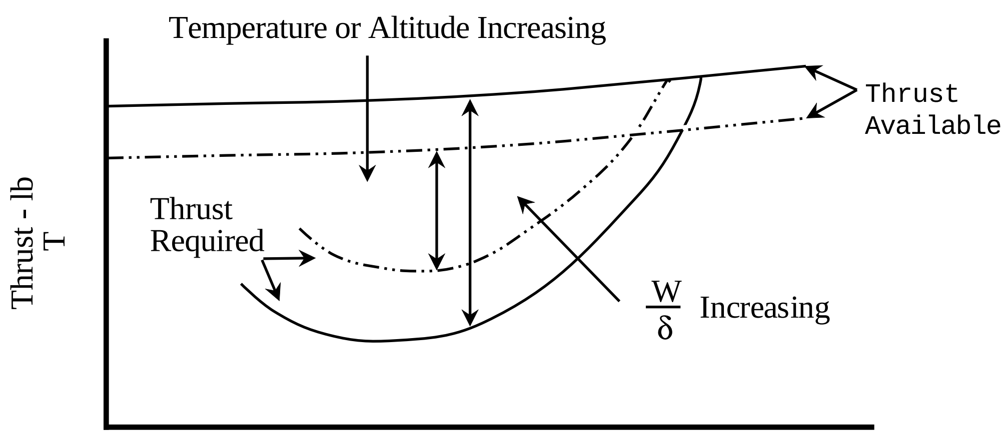

Figure 6.17
EXCESS THRUST

For stabilized level flight, thrust equals drag. At 1 g, the result is that thrust required varies with referred weight, W/δ, Mach number, and Reynold’s number. For the maneuvering case, since lift equals n_zW, the thrust required varies with n_zW/δ. Changes in W at 1 g are equivalent to changes in n_z at constant W. Figure 6.18 graphically depicts this relationship.

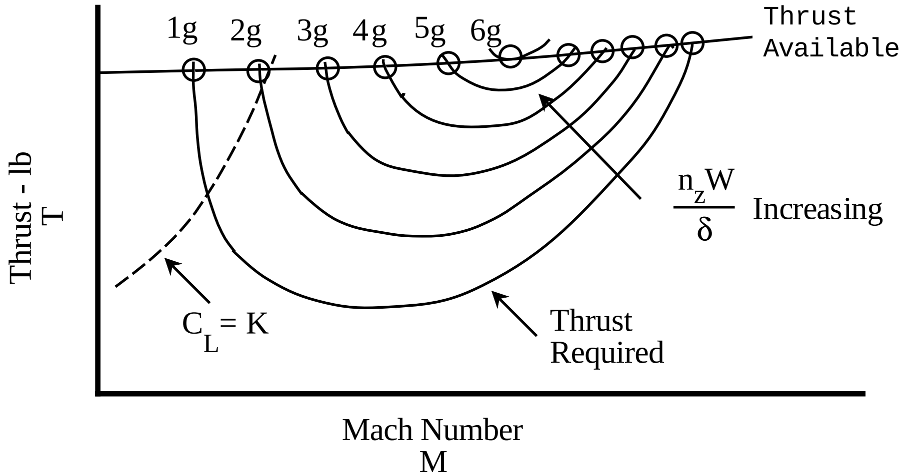

Figure 6.18
VARIATION OF EXCESS THRUST WITH LOAD FACTOR

This figure can be used to interpret the sustained turning performance. The intersections of the thrust required and available curves for various load factors indicate the airspeeds at which the airplane can sustain that load factor in a level turn. A crossplot of those intersections yields a sustained turn performance graph shown in figure 6.19.

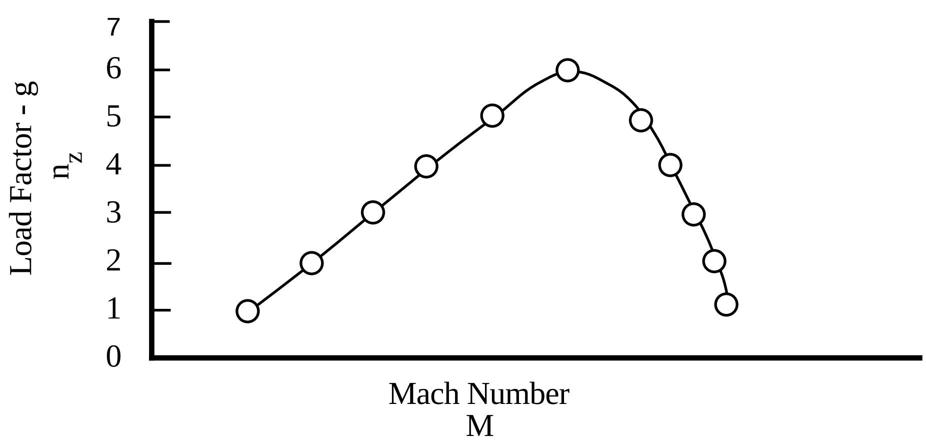

Figure 6.19
SUSTAINED TURN PERFORMANCE

6.3.5.1 SUSTAINED LOAD FACTOR

The conditions for maximum sustained load factor are found by observing in stabilized level turns, thrust equals drag. Using the general form of the drag equation:

$$D = \frac{C_D}{C_L} L \quad \text{(Eq 6.41)}$$

Substitute $n_z W$ for L, and T for D:

$$T = \frac{C_D}{C_L} n_z W \quad \text{(Eq 6.42)}$$

Rearranging:

$$n_z = \frac{T}{W} \frac{C_L}{C_D} \quad \text{(Eq 6.43)}$$

The maximum load factor results when the product of thrust-to-weight and lift-to-drag ratios is maximized. For a jet, where thrust available is assumed to be constant with velocity, the result is:

$$n_{z_{sust_{max}}} = \frac{T}{W} \left(\frac{C_L}{C_D} \right)_{max} \qquad (\text{Jet}) \quad \text{(Eq 6.44)}$$

The maximum sustained load factor occurs at the maximum lift-to-drag ratio for a jet airplane. For a propeller airplane, the result is:

$$n_z = \frac{T\left(V_T\right)}{W} \frac{L}{D\left(V_T\right)} \quad \text{(Eq 6.45)}$$

Substituting,

$$n_{z_{sust_{max}}} = \frac{THP_{avail}}{W} \frac{L}{\left(THP_{req}\right)_{min}} \qquad (\text{Propeller})$$

(Eq 6.46)

Where:

C_D	Drag coefficient	
C_L	Lift coefficient	
D	Drag	lb
L	Lift	lb
n_z	Normal acceleration	g
$n_{z\ sust\ max}$	Maximum sustained normal acceleration	g
T	Thrust	lb
THP_{avail}	Thrust horsepower available	hp
THP_{req}	Thrust horsepower required	hp
V_T	True airspeed	ft/s
W	Weight	lb.

Since thrust horsepower available is constant, the maximum sustained load factor occurs at minimum power required for a propeller airplane.

6.3.5.2 SUSTAINED TURN RADIUS AND TURN RATE

Sustained turn radius and turn rate are calculated using the following level turn equations:

$$\omega_{sust} = \frac{57.3\ g}{V_T} \sqrt{n_{z_{sust}}^2 - 1} \qquad (\text{deg/s})$$

(Eq 6.47)

And,

$$R_{sust} = \frac{V_T^{\ 2}}{g\sqrt{n_{z_{sust}}^2 - 1}}$$

(Eq 6.48)

Where:

g	Gravitational acceleration	ft/s^2
$n_{z\ sust}$	Sustained normal acceleration	g
R_{sust}	Sustained turn radius	ft
V_T	True airspeed	ft/s
ω_{sust}	Sustained turn rate	deg/s.

Typical curves for sustained turn performance are presented together with the results from instantaneous turn performance in figure 6.20.

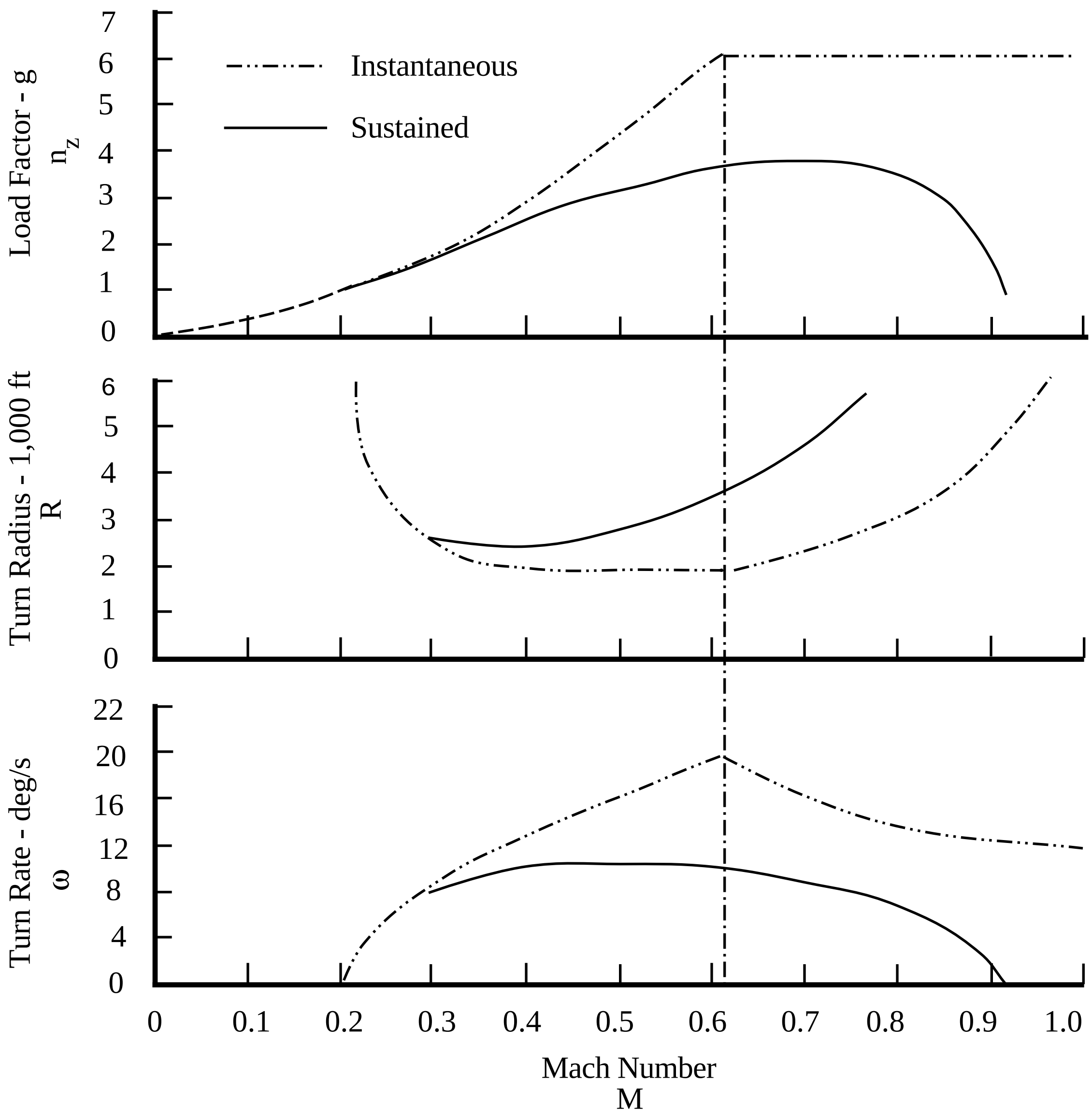

Figure 6.20

TURN PERFORMANCE CHARACTERISTICS

6.3.5.3 CORRECTIONS TO STANDARD DAY CONDITIONS

The maximum sustained load factor in a level turn is achieved when the drag balances the excess thrust at the particular flight conditions tested. Any variations in thrust available will alter the amount of drag which can be balanced. To correlate test data and refer it to standard conditions, the thrust characteristics of the engine must be known.

6.3.5.3.1 THRUST CORRECTION

Values of load factor obtained at test conditions must be corrected to account for variations in thrust from standard conditions. Measuring inflight thrust is not easy, but corrections to thrust are relatively straightforward. The procedure requires both an engine model and a drag model. Lacking either of these models, thrust correction cannot be made.

Thrust is a function of engine speed, altitude, Mach number, and ambient temperature, T_a. Analysis shows referred thrust, T/δ, has only two variables:

$$\frac{T}{\delta} = f\left(M, \frac{\dot{W}_f}{\delta_T \sqrt{\theta_T}}\right) \tag{Eq 6.49}$$

For a given airplane and engine, the maximum RPM is a constant; the thrust correction is for temperature variation alone. A typical plot of the variation of referred thrust with fuel flow referred to total conditions is presented as figure 6.21.

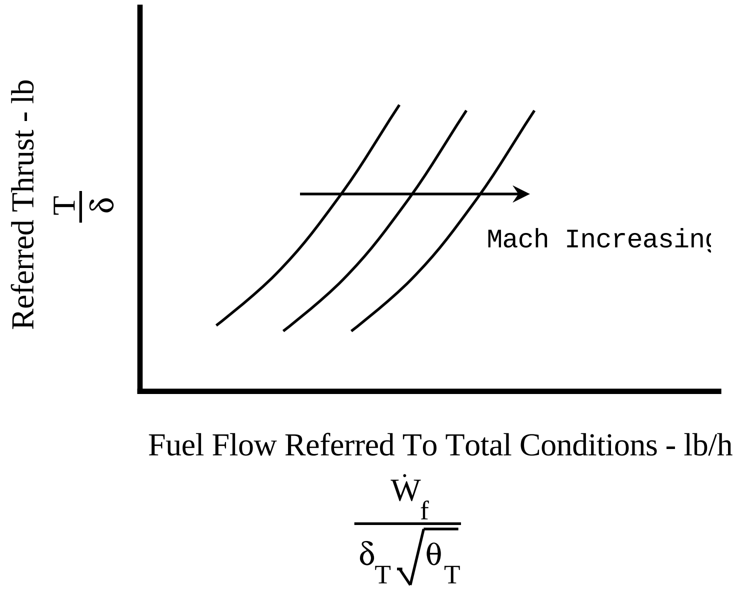

Figure 6.21
REFERRED THRUST REQUIRED

For any test Mach number, the thrust differential can be found by comparing the value of referred thrust obtained from test day referred engine speed, and referred thrust based upon the standard conditions. The difference is a function of temperature alone.

Since the thrust equals drag constraint applies to standard conditions, as well as test conditions, the difference in drag, ΔD, is identical to the thrust differential, ΔT.

$$\frac{\Delta D}{\delta} = \frac{\Delta T}{\delta} \qquad \text{(Eq 6.50)}$$

To relate the drag differential to a sustained load factor correction, the corresponding lift differential must be found. The drag model is required for this step.

The drag polar is typically determined from level flight and acceleration tests. A parabolic drag polar is shown in figure 6.22 as an example.

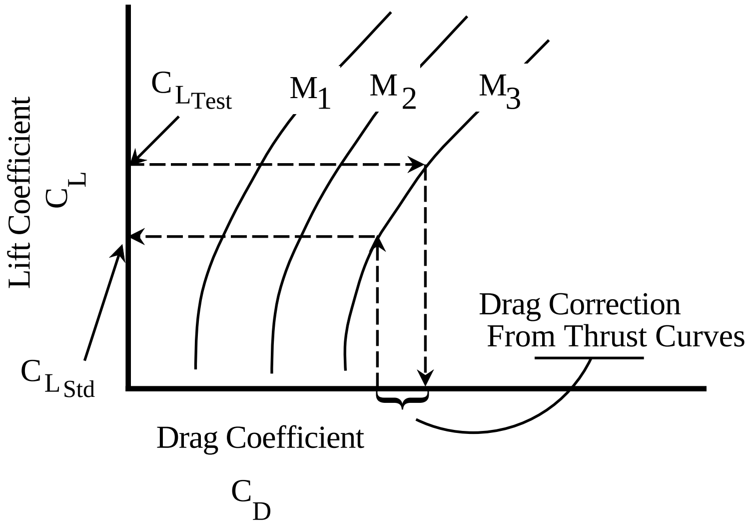

Figure 6.22
SAMPLE DRAG POLAR

For each test lift coefficient, a corresponding drag coefficient can be obtained from the drag polar. The drag differential (equal to the thrust differential) is added and the drag polar is used once again to obtain a corrected lift coefficient. Finally, the corrected lift coefficient is used to calculate the standard day load factor.

The drag correction can also be calculated if the equation for the polar is known. Given the thrust differential from the engine curves, the equivalent drag differential has this form for a parabolic drag polar:

$$\Delta D_{Std\text{-}Test} = \frac{1}{\pi e AR\, S\, (0.7)\, P_{ssl}\, \delta_{Test}\, M^2} \left[\left(n_z W\right)^2_{Std} - \left(n_z W\right)^2_{Test} \right] \quad \text{(Eq 6.51)}$$

Solving the above Eq for $n_{z\,Std}$ and substituting ΔT for ΔD,

$$n_{z_{Std}} = \sqrt{\frac{1}{W^2_{Std}} \left[\left(n_z W\right)^2_{Test} + \Delta T\, \pi\, e\, AR\, (0.7)\, S\, P_{ssl}\, \delta_{Test}\, M^2 \right]} \quad \text{(Eq 6.52)}$$

Where:

AR	Aspect ratio	
D	Drag	lb
δ	Pressure ratio	
D_{Std}	Standard drag	lb
D_{Test}	Test drag	lb
δ_{Test}	Test pressure ratio	
M	Mach number	
$\frac{N}{\sqrt{\theta}}$	Referred engine speed	RPM
n_z	Normal acceleration	g
π	Constant	
P_{ssl}	Standard sea level pressure	psf
S	Wing area	ft^2
T	Thrust	lb
W	Weight	lb.

6.3.5.3.2 GROSS WEIGHT CORRECTION

Lacking either the thrust model or the drag polar, thrust cannot be corrected. If the thrust correction to standard conditions is assumed to be zero, the drag correction and the lift differential must be zero as well. The correction to standard weight reflects the condition where lift (n_zW) is constant for the two conditions. Notice the weight correction is contained in thrust correction (in Eq 6.52, let $\Delta T = 0$):

$$n_{z_{Std}} = n_{z_{Test}} \left(\frac{W_{Test}}{W_{Std}} \right) \qquad \text{(Eq 6.53)}$$

Where:

$n_{z_{Std}}$	Standard normal acceleration	g
$n_{z_{Test}}$	Test normal acceleration	g
W_{Std}	Standard weight	lb
W_{Test}	Test weight	lb.

6.3.6 THE MANEUVERING DIAGRAM

The instantaneous and sustained performance characteristics are often displayed together on an energy maneuvering(E-M) diagram, also called a doghouse plot. Such a plot is shown in figure 6.23

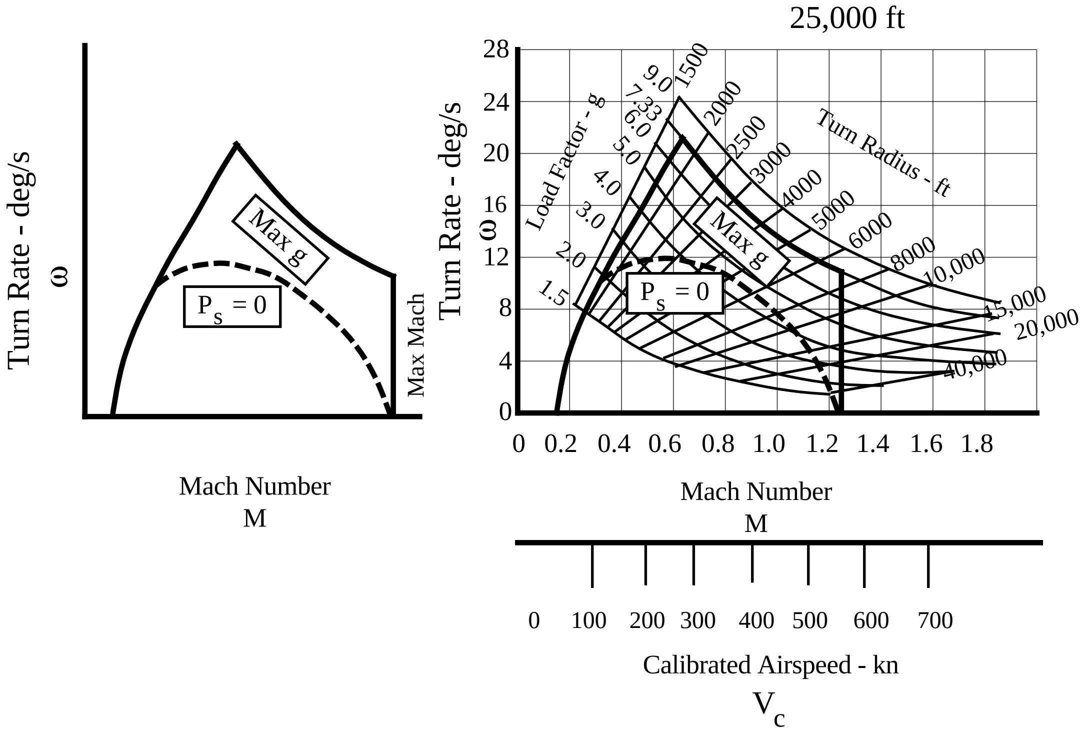

Figure 6.23
MANEUVERING DIAGRAM

In figure 6.23, the diagram grid refers to only one altitude and one weight, expressing the following relevant instantaneous and sustained turning parameters: load factor, turn radius, turn rate, Mach number, and airspeed. To plot the turn performance characteristics for another altitude, the maneuvering diagram for that altitude must be used. Notice data reduction in this format is minimal, since only one of the turn performance parameters (n_Z, R, ω) is needed to specify all three.

This diagram is extremely useful in documenting and comparing airplanes. A major weakness in this depiction, however, is it doesn't indicate performance over a time interval (except for the $P_S = 0$ condition). It doesn't show, for example, how long the instantaneous performance can be maintained. To investigate these dynamic performance characteristics, a total energy analysis is made.

6.3.7 MANEUVERING ENERGY RATE

The previous sections define and describe maneuvering performance at a constant speed. To investigate maneuvering performance when speed is changing, it is necessary to describe the relationship between linear accelerations and radial accelerations. In Chapter 5, acceleration performance was covered in detail using an energy analysis. In this and subsequent sections, the energy analysis is applied to maneuvering performance and the results are combined with acceleration performance to provide a measure of airplane agility. A brief review of energy concepts follows.

As an airplane flies, propulsive energy from the fuel is added to the total energy state of the airplane in the form of an increase in either potential or kinetic energy. When the airplane maneuvers, energy is dissipated against drag. The relative energy gain and loss characteristics of an airplane during maneuvering are important measures of its dynamic performance.

As in the 1 g case, the excess thrust characteristics determine the actual energy rate. The energy rate is observable (and measurable) as a combined instantaneous rate of climb (or descent) and flight path acceleration (or deceleration).

The maneuvering energy rate is described by the specific excess power measured while turning. Turning increases the induced drag, which decreases the excess thrust and reduces P_S. This characteristic variation of P_S with load factor is depicted in figure 6.24.

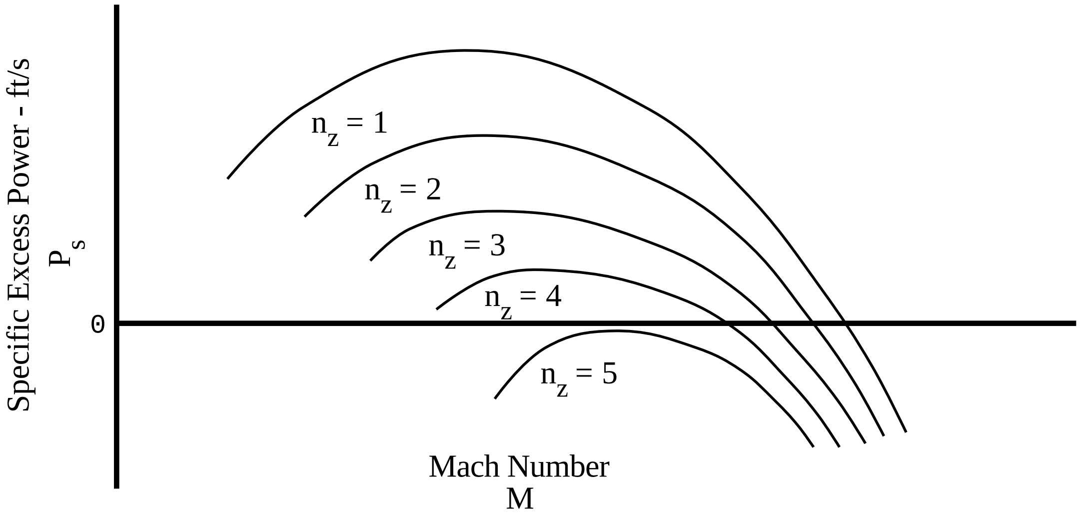

Figure 6.24

VARIATION OF SPECIFIC EXCESS POWER WITH LOAD FACTOR

Notice the similarity of figures 6.18 and 6.24. The former shows the excess thrust, while the latter shows the excess thrust times velocity divided by weight. Notice also the intercepts of the P_S curves with the horizontal axis, the points where $P_S = 0$. These points represent maximum sustained turning performance, since T = D. At all other points, there is either a thrust excess or a thrust deficit, manifested by a measurable energy rate.

6.3.8 PREDICTING TURN PERFORMANCE FROM SPECIFIC EXCESS POWER

Turning performance may be predicted from level acceleration data, using the relationship between specific excess power and the induced drag. Recall that corrections to sustained turn performance were made for thrust changes using the calculated thrust difference and the $P_S = 0$ condition (T = D) to calculate the drag differential. The differential lift was then obtained using the drag polar. Here, the excess thrust can be measured directly at each Mach number using the following:

$$T_{ex} = T - D = \frac{W}{V_T}\frac{dh}{dt} + \frac{W}{g}\frac{dV_T}{dt} \qquad \text{(Eq 6.54)}$$

Where:

D	Drag	lb
g	Gravitational acceleration	ft/s^2
h	Tapeline altitude	ft
T	Thrust	lb
T_{ex}	Excess thrust	lb
V_T	True airspeed	ft/s
W	Weight	lb.

The correction for excess thrust can be made in the same manner previously described. For this application, the excess thrust at a particular Mach number can be interpreted as the increase in drag required to make $P_S = 0$. Entering the drag polar with this drag differential, the lift differential can be found. Eq 6.51 can be used for this calculation with a parabolic drag polar. From the lift increase, the predicted maximum sustained load factor at the Mach number in question is calculated.

To compile acceleration data at many different altitudes, excess thrust (from Eq 6.54) characteristics can be documented. For a fixed altitude, referred excess thrust, T_{ex}/δ, varies with Mach number as shown below.

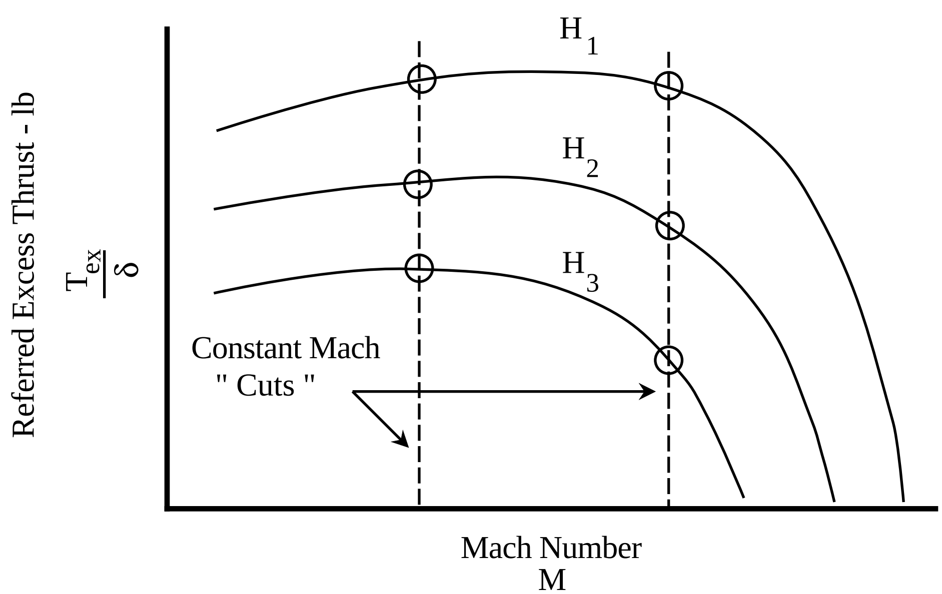

Figure 6.25
REFERRED EXCESS THRUST VERSUS MACH NUMBER

From the graph a vertical cut (at constant Mach number) yields the values representative of the drag differential at each test altitude. These values are different since the angle of attack varies across the altitude range. If the drag polar is available (or assumed of a certain order), the lift difference can be calculated, expressed as a function of referred load factor divided by Mach number times δ, all raised to the appropriate power. Figure 6.26 is a graphical depiction of this calculation.

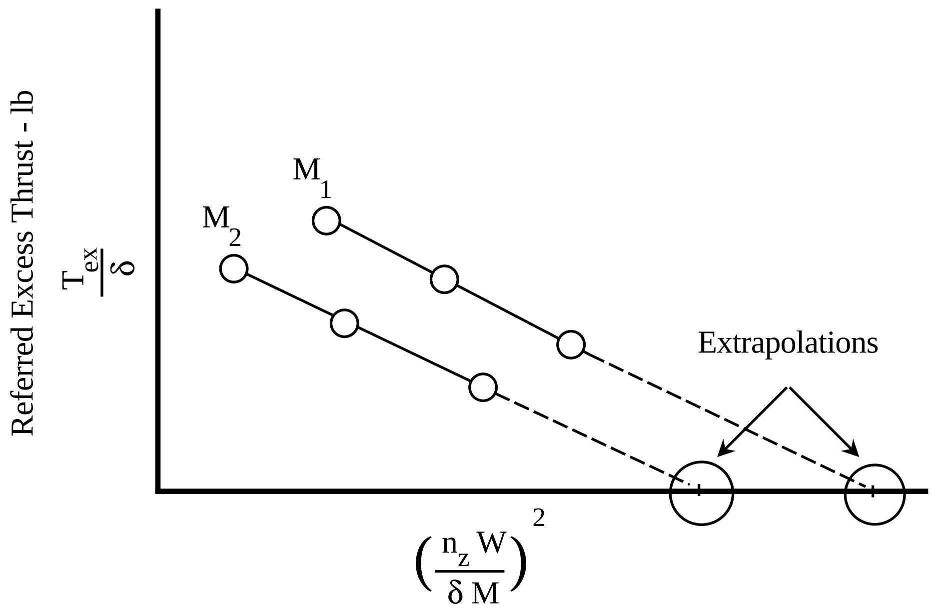

Figure 6.26
EXTRAPOLATIONS TO ZERO REFERRED EXCESS THRUST FOR A PARABOLIC DRAG POLAR

The above figure assumes a parabolic drag polar, so the data linearize to allow extrapolations to zero excess thrust, the area of interest. Each intercept defines maximum sustained load factor for a standard weight at a particular Mach number for different altitudes (because of the δ). A crossplot of sustained load factor at a standard weight versus Mach number for various altitudes can be made, as shown in figure 6.27.

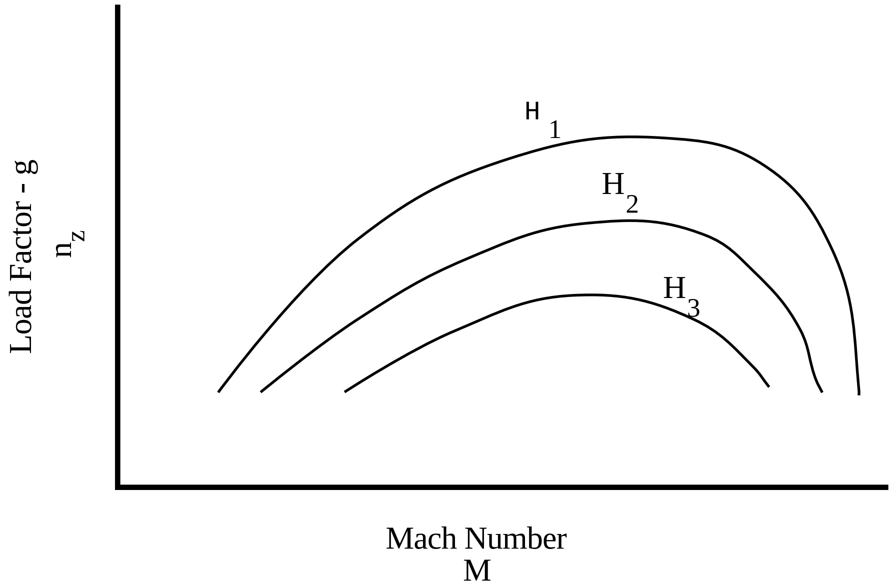

Figure 6.27
PREDICTED MAXIMUM SUSTAINED LOAD FACTOR VERSUS MACH NUMBER

6.3.9 AGILITY

Turn performance is but one aspect of an airplane's maneuvering performance. To describe the characteristics desirable in a tactical airplane, the term agility is often used. Agility is the ability to make rapid, controlled changes in airplane motion. Included within the scope of the term agility are the climb, acceleration, deceleration, and turn characteristics of the airplane. An agile airplane is capable of performing quick and precise changes in climb angle, speed, or direction of flight. The ability to make rapid changes describes maneuverability; the ability to precisely guide the airplane through such changes describes controllability. Thus, maneuverability and controllability are subsets of agility.

While it might seem reasonable to demand every airplane be agile, the concept is not practical. The cost of agility is prohibitively high, particularly for relatively large airplanes. From a design perspective, the problem is how to obtain enough thrust and control power to overcome the inertia and aerodynamic damping of the airplane. For large airplanes the problem is insurmountable with current technology. Virtually every agile airplane ever built was relatively small. Only the small airplanes are nimble at low speeds, since the control power requirements for large airplanes are so hard to meet at low speeds.

6.3.10 AGILITY COMPARISONS

Not every mission has a requirement for agility. In fact, turning performance flight tests are routinely omitted in the testing of transport and cargo category airplanes. The tactical combat airplanes are those which have a mission requirement for agility. For these airplanes, the task of specifying a particular level of agility is difficult. There is no consensus, but there are several popular ways to compare the agility of rival airplanes. Some figures of merit for these comparisons are characteristics already investigated in this and previous chapters. The formats for the comparisons differ, with each having its own advantages and disadvantages. Some of the common methods are presented in the following discussions.

6.3.10.1 SPECIFIC EXCESS POWER OVERLAYS

Using acceleration run data at various altitudes and a common load factor, contours of constant P_S can be shown on an H-V diagram. If the plots are overlaid for rival airplanes, the areas of relative P_S advantage for each are evident. An example of one such P_S overlay is shown as in figure 6.28.

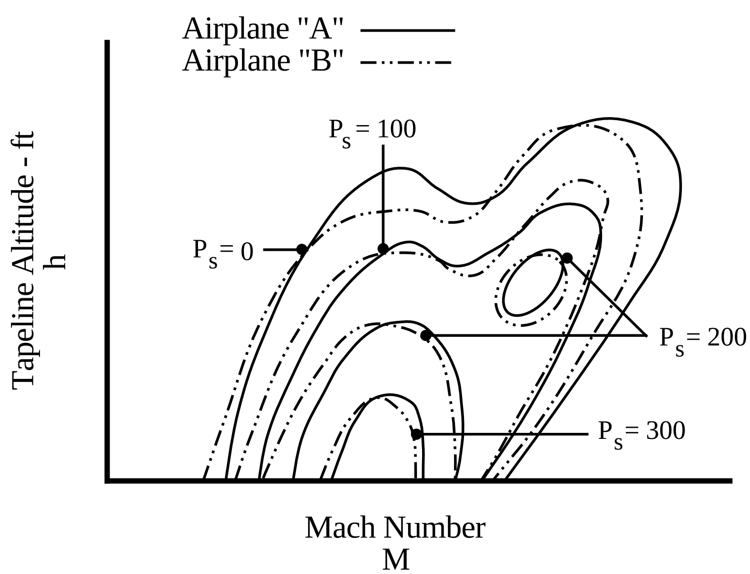

Figure 6.28
SPECIFIC EXCESS POWER OVERLAY

Careful inspection of the overlay reveals the areas of relative superiority and inferiority. But, the plot is difficult to study. If enough P_S contours are displayed to interpret the relative P_S envelopes, the plot becomes cluttered. If the relative differences are great, the plot is even harder to read. A cleaner presentation of the same data can be made by plotting only the P_S differential.

6.3.10.2 DELTA SPECIFIC EXCESS POWER PLOTS

Displaying the differential P_S of the two rival airplanes (A and B) on the H-V diagram can be a more useful format for comparing relative strengths. The delta P_S is obtained by subtracting the P_S of one airplane from the other at each energy state. Figure 6.29 is a sample delta P_S plot.

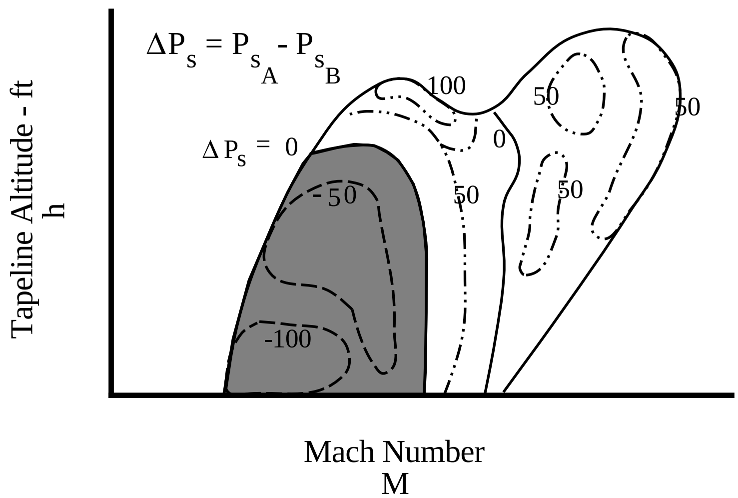

Figure 6.29
DELTA SPECIFIC EXCESS POWER CONTOURS

Areas of relative advantage are easily seen in this presentation format. For example, the shaded areas represent regions where the delta P_S is negative. For airplane A, operating in these shaded regions is discouraged, since the rival airplane (B) enjoys a P_S advantage there. Preferred energy conditions for engagements can be determined from this graph.

Unfortunately, the delta P_S plot is for one load factor. Once the airplane begins to turn, the delta P_S contours change. For a more complete representation of the tactical envelope, similar plots for other load factors are needed. These data come from loaded acceleration and deceleration tests. Composite overlays of different load factors can be used to indicate the delta P_S trends with load factor. The 2 g plot can overlay the 1 g plot, for example, to show the changing P_S situation when the airplanes begin to maneuver. A complete maneuvering picture requires overlays at regular intervals up to the limit g, but the presentation can become cluttered quickly. Another way to present the changing P_S as the airplane maneuvers uses the familiar maneuvering diagram.

6.3.10.3 DOGHOUSE PLOT

The doghouse plot maneuvering diagram, introduced in paragraph 6.3.6, is named for its characteristic shape. This diagram was used in the earlier discussion for a combined presentation of sustained and instantaneous turn performance data. The plot is also a useful display for data from loaded accelerations and decelerations. With these additional data, various P_S contours can be mapped, as figure 6.30 illustrates.

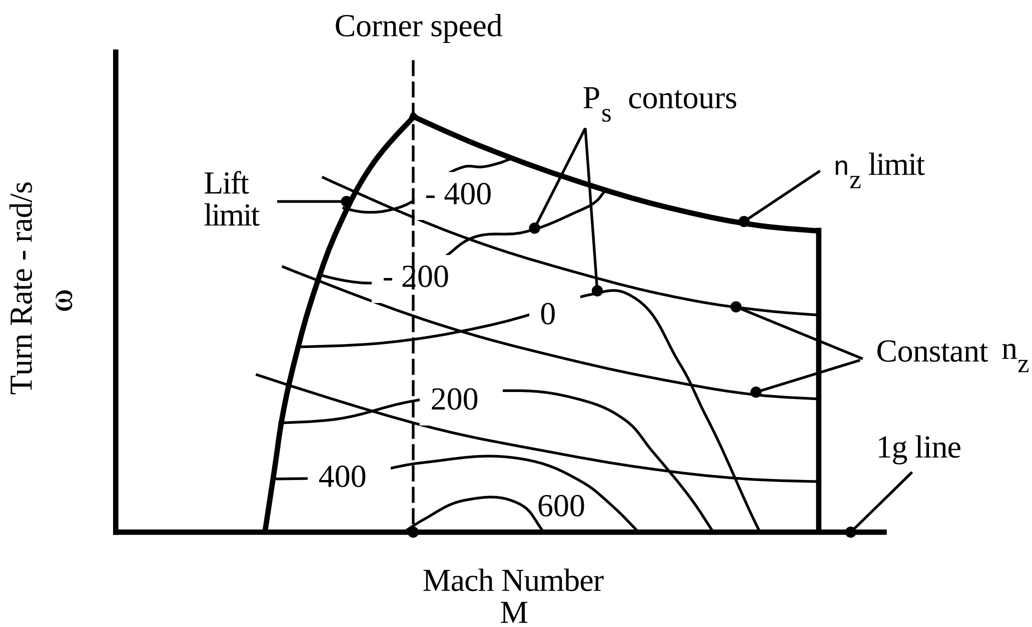

Figure 6.30
DOGHOUSE PLOT WITH SPECIFIC EXCESS POWER CONTOURS

Significant features shown on the plot include:

1. Maximum maneuver limits (stall, limit load, limit speed).
2. Corner speed.
3. Sustained turn line ($P_S = 0$).

4. Turn rate and energy loss for any speed and g.

Studying this diagram, the tactical pilot can plan his maneuvers based upon the conditions for best energy gain and energy conservation. For tactical comparisons, the diagrams for rival airplanes can be overlaid to show the areas of relative energy advantage. Like the P_S overlays, these plots can become extremely cluttered. Less cluttered versions of these displays use delta P_S contours, as in figure 6.29. A limitation of this comparison format is the reference to one altitude and weight. Many such diagrams, representing other operating conditions, must be correlated in order to put together a complete picture for tactical planning.

6.3.10.4 SPECIFIC EXCESS POWER VERSUS TURN RATE

If a vertical cut is made on a maneuvering diagram, the value of P_S can be plotted as a function of either load factor or turn rate for a constant Mach number and altitude, as shown in figure 6.31.

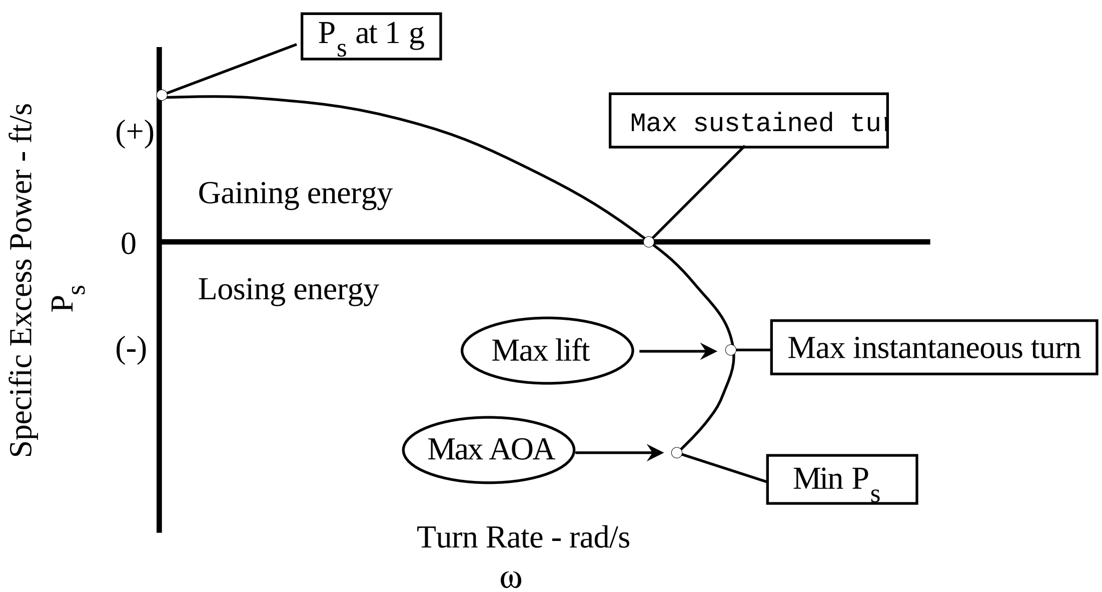

Figure 6.31
SPECIFIC EXCESS POWER VERSUS TURN RATE

This plot gives a better feel for the rate at which P_S changes as a turn is tightened. The maximum sustained turn is represented by the x axis intercept. The maximum instantaneous turn rate is an end point if the data come solely from a doghouse plot (since on a doghouse plot there is no way to show more than one value of P_S for any combination of Mach number and turn rate). However, if loaded deceleration runs are continued past the accelerated stall, the data can be used to continue this curve past the maximum instantaneous turn, to the limit angle of attack. In this case, the decreasing load factor beyond the maximum instantaneous performance point causes less turn rate, even as greater energy is sacrificed. Despite the diminished turn rate, these high energy loss conditions are tactically useful for maximum rate decelerations to force an overshoot or to take advantage of slow speed pointing ability. Inspecting the shape of the curve can reveal a point of diminishing returns, a turn rate beyond which the increase in performance does not justify the increased rate of energy loss.

The simplicity of these plots makes it relatively easy to interpret overlays for comparisons. Figure 6.32 is an example comparison using this data format.

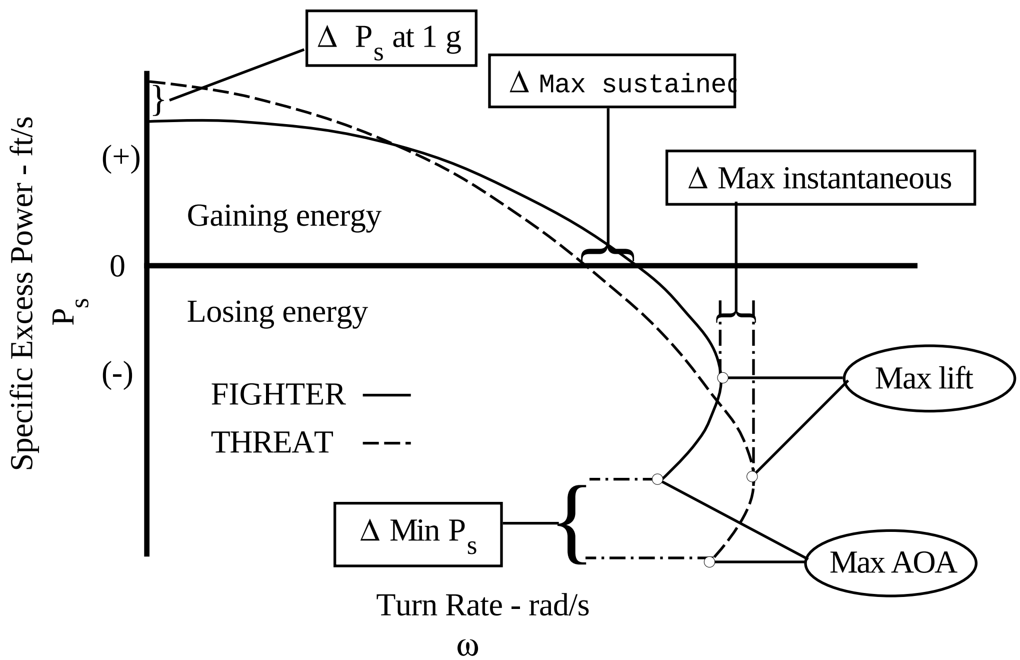

Figure 6.32
SPECIFIC EXCESS POWER VERSUS TURN RATE COMPARISON

The relative P_S advantage at any turn rate is the vertical distance between the curves. Alternately, for any P_S, the difference in turn rate capability is displayed as the horizontal spread. This presentation can be used to develop tactical maneuvers against specific rival or threat airplanes.

Still, this curve represents only one Mach number and altitude. To complete the maneuvering picture, several of these curves are required. Usually, either altitude or Mach number is fixed and the other is plotted in some carpet map format, with P_S and either turn rate or load factor. An example of such a plot is shown in figure 6.33.

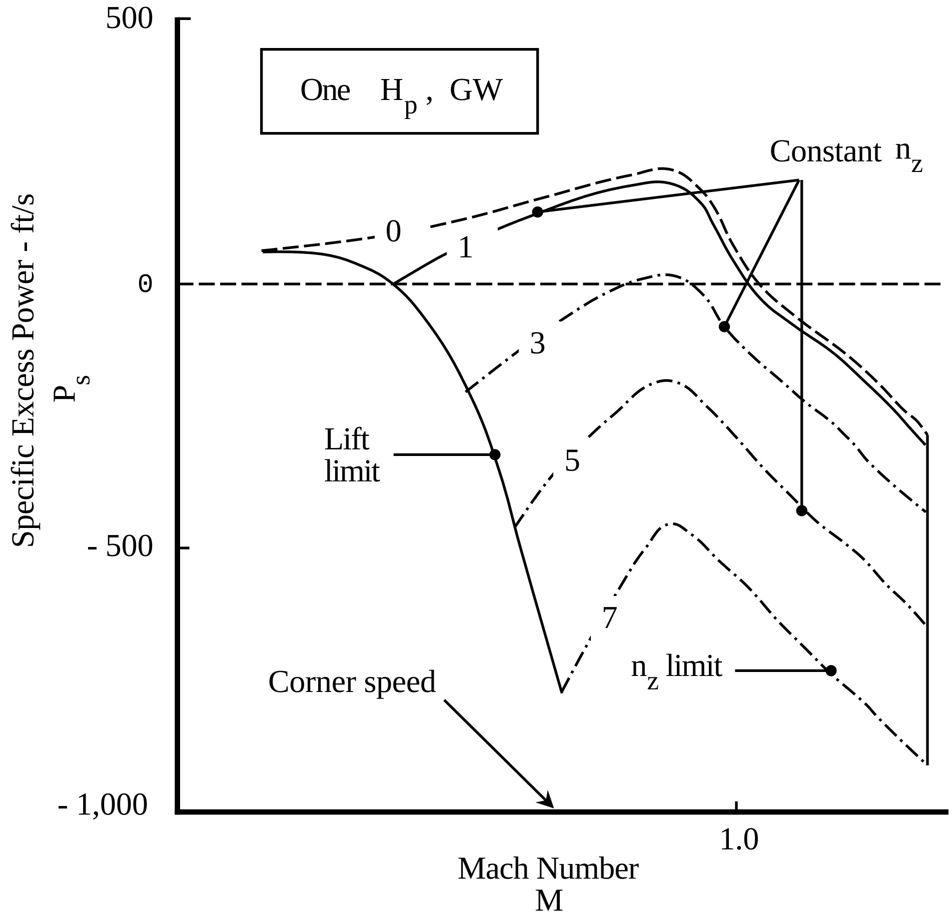

Figure 6.33
COMPOSITE MANEUVERING DIAGRAM

All of these presentations show the areas of relative P_S advantage for comparisons. They also provide data for the development of tactics against a particular rival airplane. The maneuvering environment is fluid and the airplanes don't stay on any one particular curve long enough to validate the analyses. Nevertheless, these formats serve well in the analysis of a tactical environment consisting of relatively prolonged engagements and rear-quarter attacks. In this scenario, the pilot who starts with the most energy and maintains an energy advantage throughout the engagement can wait for an opportunity to make a lethal attack, or can disengage at will.

The chief disadvantage of tactical analyses based upon these data presentations is they don't treat the quick fight. Neither do they address the capabilities of all-aspect missiles. If the opponent has the ability to make the quick kill, an analysis based upon a drawn-out energy duel is irrelevant. The quick turn at maximum performance becomes the critical parameter. While the relative energy loss rate for instantaneous maneuverability is displayed on the previously introduced plots, it's hard to visualize the overall effect of a P_S advantage or deficit. For example, using these diagrams it's difficult to interpret how fast airspeed is lost or how quickly it can be regained after a maximum performance maneuver. It also doesn't show how long a high turn rate can be maintained. One presentation which shows what happens over time is the dynamic speed turn plot.

6.3.10.5 DYNAMIC SPEED TURN PLOTS

The typical future combat confrontation will likely consist of rapid decelerations, maximum rate turning, quick shots, and maximum accelerations. In order to analyze these maximum maneuvers, a format is needed which retains the dynamic quality of the maneuvers. Dynamic speed turn plots, introduced in reference 2, are diagrams which show the potential to gain or lose airspeed in a maximum maneuver.

The first plot is constructed by converting the negative P_S values along the maximum instantaneous turn boundary into an airspeed deceleration in kn/s using Eq 6.55.

$$\frac{dV_T}{dt} = \frac{11.3 \ P_s}{V_T} \qquad \text{(Eq 6.55)}$$

Where:

P_S	Specific excess power	ft/s
V_T	True airspeed	ft/s.

Turn rate is plotted against the calculated deceleration rate, with airspeeds annotated along the resulting curve, as shown in figure 6.34.

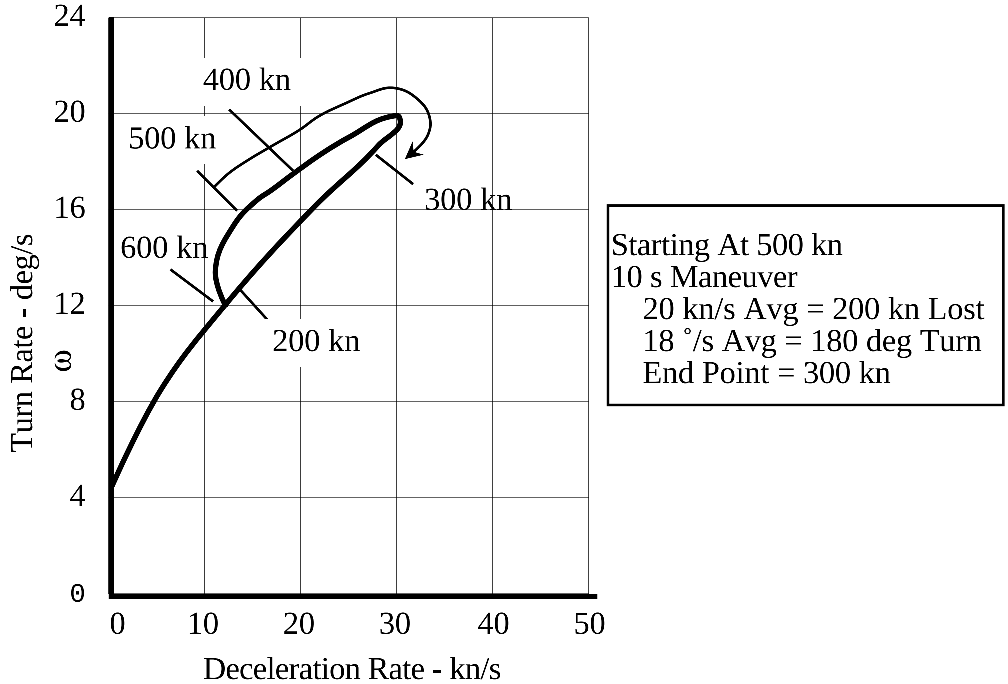

Figure 6.34
DYNAMIC TURN PLOT

This diagram can be used to visualize the dynamic performance in a maximum performance decelerating turn. The following example, extracted from reference 2, illustrates how the plot can be used. An airplane at 500 kn true airspeed begins a maximum performance turn. The average deceleration rate for the next 10 seconds is about 20 kn/s. Over the 10 second period, the airplane loses about 200 kn, while averaging about 18 deg/s turn rate. After the 180 deg turn the airplane is at 300 kn, with the capability for an instantaneous turn rate of about 18 deg/s.

The second is a plot of acceleration versus airspeed at 1 g. It can be constructed directly from 1 g acceleration run data. Accelerations are obtained from standard day data, using Eq 6.55. Acceleration is plotted against airspeed, or Mach number, as shown in figure 6.35.

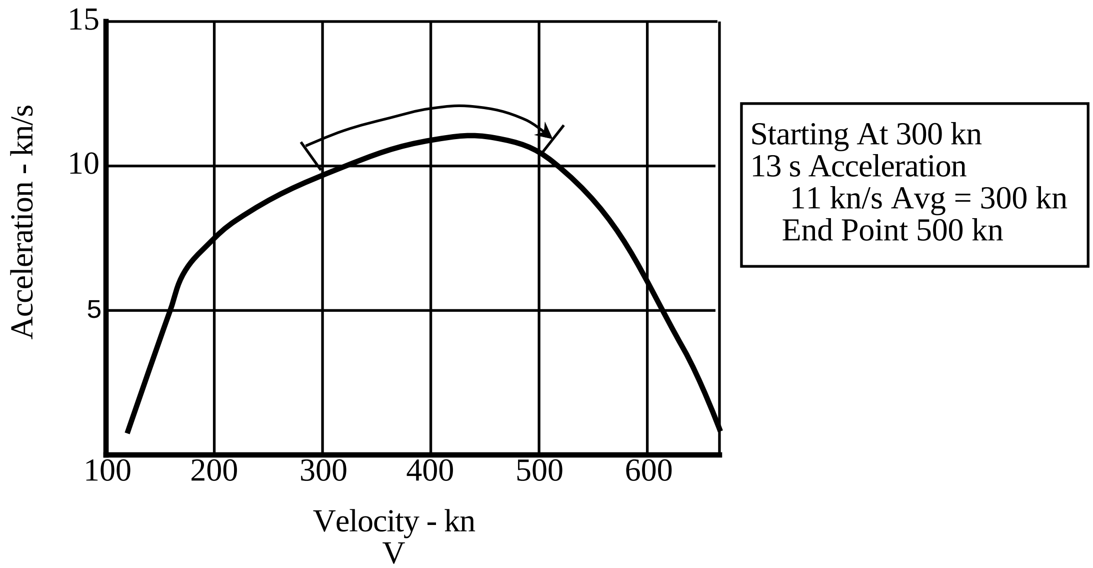

Figure 6.35
DYNAMIC SPEED PLOT

To continue the previous example, the same airplane begins a level acceleration from 300 kn to regain energy following its maximum performance turn. From 300 kn to 500 kn, the average acceleration is about 11 kn/s. The airplane is back at 500 kn after about 13 s.

The dynamic speed turn plots can be used to compare airplanes, by plotting the data of the rivals on the same graph. Quick-look analyses, as in the example above, can be made easily for a typical maneuver; computers can be used for precise analyses of capabilities.

6.4 TEST METHODS AND TECHNIQUES

The measures of maneuvering performance are turn rate, turn radius, load factor, Mach number, and altitude. All of these parameters are found on the maneuvering diagram, an example of which is presented as figure 6.36.

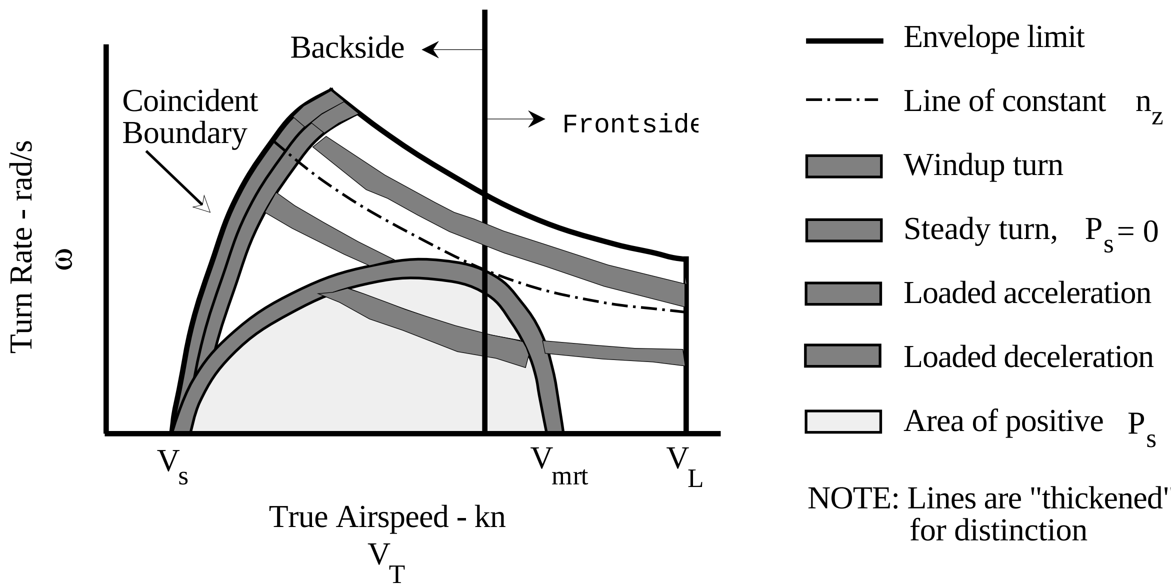

Figure 6.36
TURN PERFORMANCE CHARACTERISTICS

The diagram is helpful in describing the rationale for individual test techniques used to document maneuvering performance.

The first area of interest is the 1 g speed envelope for level flight. This is represented on the graph by the horizontal axis. The data for this boundary are normally obtained through level accelerations, as discussed in Chapter 5. Chief characteristics are the 1 g stall speed and the military rated thrust airspeed (V_{mrt}).

The boundary on the left is the lift limit. It represents accelerated stall conditions from just above the 1 g stall speed to the corner speed. Two techniques are used to document this area: windup turns and loaded decelerations. This boundary is typically a region of negative P_s.

Next, look at the sustained turn performance curve. The variation of maximum sustained load factor with Mach number is normally documented with steady turns**.** Two techniques are represented: the front side (or constant altitude) technique, and the backside (or constant airspeed) technique. Sustained turn performance can be calculated from level acceleration data. All along the sustained turn performance curve, $P_s = 0$. Above the curve P_s is negative; below it, P_s is positive.

To document the area of negative P_S between the sustained turn performance curve and the load factor limit, the loaded deceleration technique is used. The positive P_S area beneath the sustained turn performance curve is documented using the loaded acceleration technique.

6.4.1 WINDUP TURN

Instantaneous turn performance is documented usually with the windup turn technique. In this technique the load factor is smoothly and steadily increased with constant Mach number. The end point of the data run is the accelerated stall or the structural limit, whichever is reached first.

To perform the windup turn, momentarily stabilize at the desired Mach number. Set the thrust for the test as you roll into a turn and smoothly increase load factor. As load factor and drag increase, reduce the pitch attitude in order to keep Mach number constant. Use bank angle to adjust the pitch attitude. When the limit condition is reached, record the g level. Increase the load factor no faster than 1/2 g/s to minimize the effects of unsteady flow.

Buffet boundary data may be obtained using this technique. To document the buffet boundaries, the load factors at which certain levels of buffet occur are recorded. Typically, the buffet levels of interest are:

ONSET - The level of buffet first discernable is termed onset buffet. Buffet detection is easier if the load factor is applied gradually in the vicinity of the onset. Once buffet has begun, the shaking and vibrations compromise precise accelerometer readings.

TRACKING - The level of buffet beyond which no offensive tracking can reasonably be made is termed tracking buffet. Tracking limits are arbitrarily defined with respect to a particular weapon or weapon system. Defining this buffet level is difficult to standardize, since it depends largely upon opinion.

LIMIT - The buffet level which corresponds to accelerated stall is called limit buffet. The maximum load factor for the windup turn occurs at this point.

Not all airplanes have three distinct buffet levels. High lift devices, particularly leading edge devices, change the level of buffet when they are deployed. The position of all high lift devices must be noted for all data runs. Variable wing sweep also changes the buffet characteristics.

6.4.1.1 DATA REQUIRED

The windup turn data document the variations with Mach number of the lift coefficients corresponding to onset, tracking, and limit buffet levels. To investigate Reynold's number effects, data can be compared for a particular Mach number at different test altitudes. When correlating data from several altitudes, test values of n_z can be kept reasonable by taking low Mach number data at low altitude, and high Mach number data at a high test altitude. The following data are required for the windup turn:

H_{P_o}, V_o or M_o, n_{z_o}, W, α, OAT.

6.4.1.2 TEST CRITERIA

1. Steady Mach number.
2. Steady g onset, rate $\leq$ 1/2 g/s for onset buffet.

6.4.1.3 DATA REQUIREMENTS

Typical data accuracy tolerances are listed below; however, requirements may vary with available instrumentation.

1. $V_o \pm 1$ kn (most accurate method to calculate Mach number).
2. M $\pm$ 0.01 M (alternate measurement).
3. $H_{P_o} \pm 100$ ft.
4. $n_{z_o} \pm 0.05$ g, or half the smallest display increment. Readings may be difficult while in buffet.
5. W nearest hundred pounds.
6. Angle of attack as required for operational correlation.
7. OAT $\pm$ 1 ˚C.

6.4.1.4 SAFETY CONSIDERATIONS

The windup turn is an intentional approach to a limiting condition. The consequences of exceeding the limit conditions during the runs must be considered in the planning stages. Contingencies such as inadvertent stall, departure, or spin must be anticipated. Review recovery procedures, particularly in cases where reconfiguring of the airplane is required during the recovery procedure.

Address the effects of sustained buffet and high angle of attack on critical airplane systems. Emphasize engine limits and handling characteristics.

6.4.2 STEADY TURN

Sustained turning performance is documented using steady turns. The maximum load factor which can be sustained in level flight at a particular Mach number is obtained using either a front side or a backside technique.

FRONT SIDE - For speed regions where the maximum sustained g decreases as speed increases, a front side, or constant altitude, technique can be used. If a constant load factor is maintained, the airplane converges to a unique airspeed. For example, if the speed deviates to a higher value, the excess power is negative at that load factor, resulting in a deceleration. Similarly, a lower airspeed causes an acceleration due to the positive excess power. Therefore, the airplane converges to the data point if the pilot holds altitude and load factor constant.

Typically, the first data point obtained using the front side technique is V_{mrt}. This point anchors the sustained turn performance curve in the same sense it anchors the P_s versus Mach number curve (at $P_{s = 0}$) for an acceleration run. Perform a shallow dive to arrive at the test altitude at an airspeed higher than the predicted V_{mrt}. Allow the airplane to decelerate while maintaining level flight (constant load factor). The airspeed converges and stabilizes at V_{mrt}.

From V_{mrt} select a bank angle, normally from 30 to 45 degrees, and allow the airplane to decelerate at the corresponding constant load factor. Maintain level flight throughout this deceleration making all corrections smooth. Rough pitch control inputs changes the load factor and consequently the drag. Since convergence to the data point speed is decidedly slower from the low speed side, the drag from excessive pitch control activity could compromise the test results. Even though the airspeed eventually converges to the data point, it may be difficult to hold the altitude steady long enough for typical front side stabilization criteria (2 kn/min criteria from level flight performance tests). If the corrections for altitude variations are smooth, the interchange between potential and kinetic energies even out over the required time interval. A good visual horizon is required, unless the airplane is equipped with an inertial system and head-up display. The flight path vector and inertial horizon simplify this technique greatly. An autopilot with an altitude hold feature can be helpful for the front side points.

At higher bank angles, altitude is difficult to control using smooth pitch control inputs alone. Figure 6.37 illustrates the variation of normal acceleration with bank angle in a steady turn.

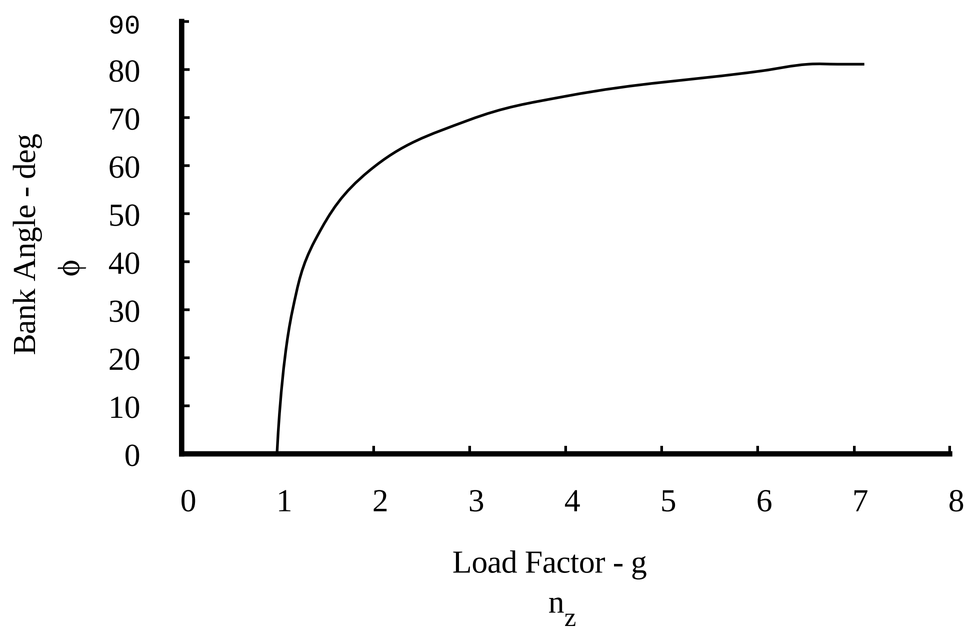

Figure 6.37
LEVEL TURN BANK ANGLE VERSUS LOAD FACTOR

Up to about 45 deg, the bank angle is a sensitive indicator of load factor. Most of the lift force is directed vertically, so small changes in load factor are effective in correcting rate of climb or descent. Above 60 deg, load factor is extremely sensitive to even small variations in bank angle. Since only a small component of the lift is directed vertically, flight path corrections with constant bank angle require excessive load factor deviations, compromising the data. For these conditions, it helps to trim to the desired load factor, using the accelerometer for reference. Bank angle can then be used to make the pitch attitude adjustments required to maintain level flight. The front side technique is practical to only about 3 g, above which the backside technique is normally used.

BACKSIDE - The backside technique is used above about 3 g, and wherever the maximum sustained g decreases as speed decreases. If a constant load factor is held in this region, the airspeed diverges from trim. For example, if the airplane gets slow, the excess power is negative and the airplane decelerates. Similarly, an airspeed faster than trim produces an acceleration. A constant airspeed technique is required since the test point is steady, but unstable.

To perform the backside technique, first stabilize at, or slightly slower than, the target airspeed. Roll into a turn and smoothly increase the thrust, while simultaneously increasing the load factor to prevent acceleration. Monitor the airspeed closely and correct deviations by adjusting the load factor. For increasing speed, apply more load factor. Fast deviations must be corrected immediately when stabilizing on the backside, since the amount of additional g required to decelerate increases with airspeed. If the airspeed deviation is too large for a comfortable correction, reduce thrust slightly to decelerate while holding the g, and then reset the thrust when the target airspeed is reached. Corrections for decreasing airspeed are easier, since accelerations can be made by a slight relaxation of load factor. While holding a steady load factor, maintain level flight by using bank angle to make fine adjustments to pitch attitude. Large pitch attitude corrections complicate or even prevent stabilization. Make a fine adjustment to the load factor when correcting for a rate of climb or descent. After the airspeed stabilizes, record the data when the airspeed, altitude, and load factor are steady for 5 seconds.

A modification of the above technique can be used for afterburner points. The rapid increase in airspeed which accompanies afterburner light off can be anticipated by initially stabilizing 20 to 30 kn slower than the desired test airspeed. After the burner lights off, the target airspeed can be intercepted with a smooth application of load factor.

As with the front side technique, a good visual horizon reference is required, but may be compensated for by a head-up display of inertial data.

6.4.2.1 DATA REQUIRED

Sustained turn performance is documented by performing level turns from V_{min} to V_{max} at constant test altitudes from near sea level to the combat ceiling of the airplane. The typical altitude interval is 5,000 ft. The following data are required for the steady turn.

H_{P_o}, V_o or M_o, n_{z_o}, W, α, OAT.

Data points should span the airspeed envelope, with a regular interval between data points. A rough plot of n_z versus airspeed or Mach number can be kept while obtaining the data as a guide to avoiding holes in the coverage.

The measurement of normal acceleration is critical for these tests. A sensitive g-meter is typically used. As discussed in previous chapters, the instrument correction is noted for 1.0 g. Then, at 1 g inflight, determine the tare correction as the difference between the actual reading and 1 g plus the instrument correction. This tare correction must be applied to each n_z reading after instrument corrections are applied.

$$n_z = n_{z_o} + \Delta n_{ic} + \Delta n_{z_{tare}} \qquad \text{(Eq 6.56)}$$

Where:

n_z	Normal acceleration	g
n_{z_o}	Observed normal acceleration	g
Δn_{ic}	Normal acceleration instrument correction	g
$\Delta n_{z\,tare}$	Normal acceleration tare correction	g.

6.4.2.2 TEST CRITERIA

1. Constant thrust.
2. Constant altitude ± 1,000 ft of target, and steady for 5 s.
3. Constant normal acceleration (bank angle).
4. Airspeed < 2 kn change over a one minute interval; steady for 5 s.

6.4.2.3 DATA REQUIREMENTS

Typical data accuracy tolerance are listed below; however, requirements may vary with available instrumentation.

1. H_{P_o} ± 100 ft.
2. V_o ± 1 kn.
3. n_{z_o} ± 0.05 g, or half the smallest display increment. Value can be calculated from the stabilized bank angle.
4. Weight ± 100 lb.
5. OAT ± 1° C.

6.4.2.4 SAFETY CONSIDERATIONS

There are no particular hazards associated with steady turns, apart from the case where the sustained and instantaneous boundaries coincide. Such conditions are covered in the previous sections. If many data points are planned, adverse effects of sustained high engine operating temperatures should be anticipated.

6.4.3 LOADED ACCELERATION

Level accelerations were introduced in Chapter 5 as a method to document the maximum thrust P_S characteristics of the airplane at 1 g. The airplane has excess thrust at higher load factors as well, but only within certain airspeed ranges, and only up to the maximum sustained load factor at the test altitude. Within these boundaries, acceleration tests can be performed while turning. The airspeed range for the loaded acceleration decreases from the 1 g envelope to a single point at the maximum sustained load factor at the test altitude. As in other dynamic test techniques, automatic data recording is necessary. Details of the 1 g level acceleration test technique are presented in Chapter 5. Loaded accelerations are performed slightly differently, as presented below.

Like the 1 g acceleration run, begin the loaded acceleration with the thrust stabilized at military or maximum thrust, depending upon the test. Choose a test load factor (half-g increments is a typical choice) and calculate the stall speed at that load factor. The initial airspeed should be 1.1 times the predicted stall speed, or higher as necessary, to ensure positive P_S for the acceleration. Begin the test below the test altitude by stabilizing the airspeed, thrust, and load factor in a slight climb. As in the 1 g acceleration, use a combination of drag devices, flaps, and climb angle as required to control the rate of climb. As the test altitude is approached, activate the test instrumentation, retract the drag devices and over-bank as necessary to intercept a level flight path. During the run, it is critical to keep the load factor constant. Small altitude variations can easily be accounted for in the data reduction, but load factor excursions compromise the data. A good way to minimize load factor excursions is to trim the pitch forces during the acceleration, provided the trim sensitivity is suitable. Adjust the bank angle to make pitch attitude corrections for level flight. Continue the acceleration until the airspeed stabilizes at the maximum sustained speed for the test load factor.

6.4.3.1 DATA REQUIRED

The following data are required from roughly 1.1 $V_{s(nz\ Test)}$ to $V_{mrt(nz\ Test)}$.

1. Pressure altitude versus time trace.
2. Airspeed versus time trace.
3. Load factor versus time trace.
4. Ambient temperature.
5. Fuel flow (integrated over elapsed time to compute change in weight).
6. Fuel weight.

6.4.3.2 TEST CRITERIA

1. Constant thrust.
2. Constant altitude ± 1,000 ft of target altitude.
3. Constant load factor ± 0.2 g.

6.4.3.3 DATA REQUIREMENTS

Typical data accuracy tolerances are listed below; however, requirements may vary with available instrumentation.

1. H_{P_o} ± 100 ft.
2. V_o ± 1 kn.
3. n_{z_o} ± 0.1 g.

4. OAT ± 1 ˚C.
5. Fuel flow ± 500 lb/h.
6. Weight ± 100 lb.

6.4.3.4 SAFETY CONSIDERATIONS

Loaded accelerations begin near the stall, so guard against the inadvertent stall while setting up the run. If speedbrakes or flaps are used prior to intercepting the acceleration profile, take care not to overspeed or over stress them.

6.4.4 LOADED DECELERATION

The loaded deceleration is used to document the region of negative P_S outside of the sustained performance curve. Decelerations can be performed from V_{Limit}, at various load factors from 1 up to the structural load limit. Decelerations performed at load factors below the maximum sustained g for the test altitude terminate on the sustained performance curve. For load factors above the maximum sustained g at the test altitude, the deceleration terminates at the lift limit. Once the lift limit is reached, the load factor is progressively relaxed so as to decelerate along the lift limit to 1 g.

If the full envelope is to be documented, begin the loaded deceleration from a shallow dive at V_{Limit} with the thrust stabilized at military (or maximum) thrust. As the test altitude is approached, activate the test instrumentation and smoothly level off, setting the target load factor and bank angle to maintain level flight. For low load factors, the deceleration will terminate on the sustained turn performance boundary. The final stages of this deceleration is precisely the front side technique used to define the sustained turn performance boundary. For load factors which exceed the sustained performance capability at the test conditions, the deceleration will continue to the accelerated stall. After the lift limit is reached, the test can be terminated. Alternately, the deceleration can be continued to document the lift limit boundary. The deceleration rate along the lift boundary is typically high, however, and the bank angle must be reduced as load factor decreases or else a high rate of descent will develop.

6.4.4.1 DATA REQUIRED

The following data are required from V_{Limit} (or, as desired) to $V_{s(nz\ test)}$.

1. Pressure altitude versus time trace.
2. Airspeed versus time trace.
3. Load factor versus time trace.
4. Ambient temperature.
5. Fuel flow (integrated over elapsed time to compute change in weight).
6. Fuel weight.

6.4.4.2 TEST CRITERIA

1. Constant thrust.
2. Constant altitude.
3. Constant load factor.

6.4.4.3 DATA REQUIREMENTS

Typical data accuracy tolerances are listed below; however, requirements may vary with available instrumentation.

1. $H_{P_o} \pm 100$ ft.
2. $V_o \pm 1$ kn.
3. $n_{z_o} \pm 0.1$ g.
4. OAT ± 1 ˚C.
5. Fuel flow ± 500 lb/h.
6. Weight ± 100 lb.

6.4.4.4 SAFETY CONSIDERATIONS

The loaded deceleration begins at high speed, where the pitch control may be sensitive and the limit load factor relatively easy to reach. Exercise care to avoid over stresses during the rapid onset of load factor at the start of the run.

The decelerations may take a relatively long time to complete, and the sustained high load factors become a physiological concern. Test planning for the high g events should address techniques to avoid the adverse effects of rapid g onset and sustained high g.

The high negative P_S near the end of the high g decelerations may result in rapid approaches to stalled conditions, so the possibility of inadvertent stalls or departures must be considered. Potential adverse effects on airplane systems from sustained buffet should be anticipated. High angle of attack engine characteristics should be studied for potential problem areas, such as compressor stall, over-temperature, and flameout.

6.4.5 AGILITY TESTS

Tests which highlight the agility of an airplane are those which document rapid transitions between states. The states include attitudes, rates, and flight path accelerations. Since agility includes the ability to precisely control these transitions, some agility test techniques are more flying qualities tests than performance tests. There is a distinction between: 1) the ability to generate a change, and 2) the ability to capture the desired final state. The distinction is between what is called transient agility and functional agility. The former describes the quickness from steady-state to a steady rate of change; the latter, from one steady state to another. The emphasis is strongly on time as a figure of merit. Evidence suggests the quickest time between states is not always accomplished with full deflection control inputs.

6.4.5.1 PITCH AGILITY

These tests highlight the nose-pointing capability of the airplane. Rapid pitch attitude changes are evaluated for 30, 60, 90, and 180 deg. The changes are made in the horizontal and vertical planes. Measures include time to maximum steady pitch rate and time to capture the final pitch angle. If automatic data recording is not available, the time to final state can be measured using a stopwatch.

6.4.5.2 LOAD FACTOR AGILITY

These tests are concerned with controlling the flight path. Wings-level roller coaster maneuvers are performed to capture prescribed load factors. The maneuvers may also be performed in the vertical plane, but energy loss rate complicates the technique. These g capture maneuvers have proved difficult to perform using digital normal acceleration displays. Digital displays can be read only when the normal acceleration is relatively steady, offering no trend information to help in the aggressive capture of precise g levels.

6.4.5.3 AXIAL AGILITY

Tests for axial agility include accelerations and decelerations using military and maximum thrust, speedbrakes, and thrust reversing. Engine spool-up time is included in the measurements. Relevant tests include decelerations from high supersonic speed to corner speed and accelerations to corner speed following a post-stall maneuver.

6.5 DATA REDUCTION

6.5.1 WINDUP TURN

The data reduction for windup turns uses the following equations:

$$V_i = V_o + \Delta V_{ic} \qquad \text{(Eq 6.57)}$$

$$V_c = V_i + \Delta V_{pos} \qquad \text{(Eq 6.58)}$$

$$H_{P_i} = H_{P_o} + \Delta H_{P_{ic}} \qquad \text{(Eq 6.59)}$$

$$H_{P_c} = H_{P_i} + \Delta H_{pos} \qquad \text{(Eq 6.60)}$$

$$n_{z_i} = n_{z_o} + \Delta n_{z_{ic}} \qquad \text{(Eq 6.61)}$$

$$n_{z_{Test}} = n_{z_i} + \Delta n_{z_{tare}} \qquad \text{(Eq 6.62)}$$

$$C_{L_{max_{Test}}} = \frac{n_{z_{Test}} W_{Test}}{0.7 P_{ssl} \delta_{Test} M^2 S} \qquad \text{(Eq 6.63)}$$

$$V_T = a\ M \tag{Eq 6.64}$$

$$R = \frac{V_T^2}{g\sqrt{\left(n_z^2 - 1\right)}} \tag{Eq 6.12}$$

$$\omega = \frac{V_T}{R} \tag{Eq 6.13}$$

Where:

a	Speed of sound	ft/s
$C_{L_{max_{Test}}}$	Test maximum lift coefficient	
$\Delta H_{P_{ic}}$	Altimeter instrument correction	ft
ΔH_{pos}	Altimeter position error	ft
$\Delta n_{z_{ic}}$	Normal acceleration instrument correction	g
$\Delta n_{z_{tare}}$	Accelerometer tare correction	g
δ_{Test}	Test pressure ratio	
ΔV_{ic}	Airspeed instrument correction	kn
ΔV_{pos}	Airspeed position error	kn
H_{P_c}	Calibrated pressure altitude	ft
H_{P_i}	Indicated pressure altitude	ft
H_{P_o}	Observed pressure altitude	ft
M	Mach number	
$n_{z\ Test}$	Test normal acceleration	g
n_{z_i}	Indicated normal acceleration	g
n_{z_o}	Observed normal acceleration	g
P_{ssl}	Standard sea level pressure	2116.217 psf
R	Turn radius	ft
S	Wing area	ft^2
V_c	Calibrated airspeed	kn
V_i	Indicated airspeed	kn
V_o	Observed airspeed	kn
V_T	True airspeed	ft/s
ω	Turn rate	rad/s
W_{Test}	Test Weight	lb.

For onset, tracking, and limit buffet levels compute C_L using the observed airspeed, pressure altitude, normal acceleration, and fuel weight. Calculate referred n_z for later analysis.

Step	Parameter	Notation	Formula	Units	Remarks
1	Observed airspeed	V_o		kn	
2	Airspeed instrument correction	ΔV_{ic}		kn	Lab calibration
3	Indicated airspeed	V_i	Eq 6.57	kn	
4	Airspeed position error	ΔV_{pos}		kn	Flight calibration
5	Calibrated airspeed	V_c	Eq 6.58	kn	
6	Observed pressure altitude	H_{P_o}		ft	
7	Altimeter instrument correction	$\Delta H_{P_{ic}}$		ft	Lab calibration
8	Indicated pressure altitude	H_{P_i}	Eq 6.59	ft	
9	Altimeter position error	ΔH_{pos}		ft	Flight calibration
10	Calibrated pressure altitude	H_{P_c}	Eq 6.60	ft	
11	Mach number	M			$f\ (H_{P_c}, V_c)$
12	Observed normal acceleration	n_{z_o}		g	
13	Normal acceleration instrument correction	$\Delta n_{z_{ic}}$		g	Lab calibration
14	Indicated normal acceleration	n_{z_i}	Eq 6.61	g	
15	Normal acceleration tare correction	$\Delta n_{z_{tare}}$		g	Flight observation
16	Test normal acceleration	$n_{z\ Test}$	Eq 6.62	g	
17	Test weight	W_{Test}		lb	
18	Test pressure ratio	δ_{Test}			$f\ (H_{P_c})$

19	Standard sea level pressure	P_{ssl}		psf	2116. psf
20	Wing area	S		ft^2	Airplane data
21	Test maximum lift coefficient	$C_{L_{max_{Test}}}$	Eq 6.63		
22	Test referred normal acceleration	$n_z \frac{W}{\delta}$		g-lb	
23	Speed of sound	a		ft/s	From Appendix VI
24	True airspeed	V_T	Eq.6.72	ft/s	
25	Turn radius	R	Eq.6.12	ft	
26	Turn rate	ω	Eq.6.13	rad/s	

6.5.2 STEADY TURN

6.5.2.1 STABILIZED TURN

Follow the data reduction in section 6.5.1 through step number 20. Corrections to standard conditions are illustrated for a parabolic drag polar, using the following equations:

$$\Delta T = T_{Std} - T \quad \text{(Eq 6.65)}$$

$$n_{z_{Std}} = \sqrt{\frac{1}{W^2_{Std}} \left[\left(n_z W\right)^2_{Test} + \Delta T \, \pi \, e \, AR \, (0.7) \, S \, P_{ssl} \, \delta_{Test} \, M^2 \right]} \quad \text{(Eq 6.52)}$$

$$V_T = a \; M \quad \text{(Eq 6.64)}$$

$$R = \frac{V_T^2}{g \sqrt{\left(n_z^2 - 1\right)}} \quad \text{(Eq 6.12)}$$

$$\omega = \frac{V_T}{R} \quad \text{(Eq 6.13)}$$

Where:

a	Speed of sound	ft/s
AR	Aspect ratio	
ΔT	Change in thrust	lb
e	Oswald's efficiency factor	
M	Mach number	
$n_{z\ Std}$	Standard normal load factor	g
R	Turn radius	ft
T	Thrust	lb
T_{Std}	Standard thrust	lb
V_T	True airspeed	ft/s
ω	Turn rate	rad/s
W_{Std}	Standard weight	lb.

The thrust correction is made according to the following steps. With the standard day n_z, the standard day turn radius and turn rate can be calculated.

Step	Parameter	Notation	Formula	Units	Remarks
1	Test temperature ratio	θ_{Test}			f (T_a)
2	Engine RPM	N		rpm	
3	Referred RPM	$\frac{N}{\sqrt{\theta}}$			
4	Thrust	T		lb	From engine curves
5	Standard temperature ratio	θ_{Std}			From Appendix VI
6	Standard referred RPM	$\frac{N}{\sqrt{\theta_{Std}}}$		rpm	
7	Standard thrust	T_{Std}		lb	From engine curves
8	Change in thrust	ΔT	Eq.6.73	lb	
9	Standard load factor	$n_{z\ Std}$	Eq.6.52		
10	Speed of sound	a		ft/s	From Appendix VI
11	True airspeed	V_T	Eq.6.72	ft/s	
12	Turn radius	R	Eq.6.12	ft	
13	Turn rate	ω	Eq.6.13	rad/s	

6.5.2.2 LEVEL ACCELERATION

The following equations are used to reduce acceleration data for the prediction of steady turn performance:

$$V_T = a\ M \qquad \text{(Eq 6.64)}$$

$$n_{z_{sust}} = \sqrt{\frac{P_{s_{1g}}\ \pi\ e\ AR\ S\ \ 0.7\ P_{ssl}\delta\ M^2}{V_T W_{Std}} + 1} \qquad \text{(Eq 6.66)}$$

$$T_{ex} = T - D = \frac{W_{Std}}{V_T}\ P_{s_{1g}} \qquad \text{(Eq 6.67)}$$

$$n_{z_{sust}} = \sqrt{\left(\frac{n_z W_{Std}}{\delta\, M}\right)^2}\ \ \frac{\delta_h}{W_{Std}}\ M \qquad \text{(Eq 6.68)}$$

Where:

a	Speed of sound	ft/s
AR	Aspect ratio	
D	Drag	lb
δ	Pressure ratio	
δ_h	Pressure ratio for selected altitude	
e	Oswald's efficiency factor	
M	Mach number	
n_z	Normal acceleration	g
$n_{z_{sust}}$	Sustained normal acceleration	g
$P_{s\ 1g}$	Specific excess energy at 1 g	ft/s
P_{ssl}	Standard sea level pressure	2116 psf
S	Wing area	ft^2
T	Thrust	lb
Tex	Excess thrust	lb
V_T	True airspeed	ft/s
W_{Std}	Standard weight	lb.

The data required from acceleration runs include P_s values for standard conditions, at specific Mach number for a given weight and altitude. Sustained normal acceleration can be calculated, or determined graphically if at least two altitudes are documented. One method to calculate $n_{z_{sust}}$ follows this sequence:

Step	Parameter	Notation	Formula	Units	Remarks
1	Specific excess power at 1 g	$P_{s\ 1\ g}$		ft/s	From acceleration run
2	Mach number	M			From acceleration run
3	True airspeed	V_T	Eq 6.64	ft/s	
4	Standard weight	W_{Std}		lb	
5	Sustained normal acceleration	$n_{z_{sust}}$	Eq 6.66	g	

For graphical data reduction, use $P_{s\ 1\ g}$ data for standard conditions at one altitude at a time. Perform steps 1 - 4 above, plus the following steps:

Step	Parameter	Notation	Formula	Units	Remarks
5	Excess thrust	T_{ex}	Eq 6.67	lb	
6	Pressure ratio	δ			f (H_{P_c})
7	Referred excess thrust	$\dfrac{T_{ex}}{\delta}$		lb	

Plot $\dfrac{T_{ex}}{\delta}$ versus Mach number for each altitude, on the same graph.

Make a vertical cut for several values of Mach number, and at each intersection record $\dfrac{T_{ex}}{\delta}$ and calculate $\left[\dfrac{n_z W_{Std}}{\delta M}\right]^2$ (here, $n_z = 1$). The exponent identifies a parabolic drag polar.

Construct a new graph of $\dfrac{T_{ex}}{\delta}$ versus $\left[\dfrac{n_z W_{Std}}{\delta M}\right]^2$ and plot the values for each Mach number chosen.

Each Mach number line can be extrapolated to the horizontal axis, representing T_{ex} = 0 at that Mach number. The value of $\left[\frac{n_z W_{Std}}{\delta M}\right]^2$ at the x axis intercept provides $n_{z_{sust}}$ data for any altitude chosen at that Mach number, as follows:

Step	Parameter	Notation	Formula	Units	Remarks
8	Pressure ratio	δ_h			For selected altitude
9	Sustained load factor	$n_{z_{sust}}$	Eq 6.68	g	

Finally, the values of $n_{z_{sust}}$ at each selected altitude can be plotted on a graph of n_z versus Mach number. The values of $n_{z_{sust}}$ at each altitude for different Mach numbers can be faired to complete the data reduction.

6.5.3 LOADED ACCELERATION

The data reduction for loaded accelerations is identical to the procedure described in Chapter 5. Final results include P_s measurements as a function of Mach number.

6.5.4 LOADED DECELERATION

Data reduction for loaded decelerations is the same as for accelerations, except the values of P_s are negative. Final results include P_s measurements as a function of Mach number.

6.5.5 AGILITY TESTS

Agility test data consists primarily of traces or simple time measurements. No standard data reduction procedure is currently specified.

6.6 DATA ANALYSIS

6.6.1 WINDUP TURN

Instantaneous turn performance parameters can be documented using the C_L data from the windup turns. Begin the analysis by plotting values of C_L for onset, tracking, and limit buffet versus Mach number. A typical plot is shown in figure 6.38.

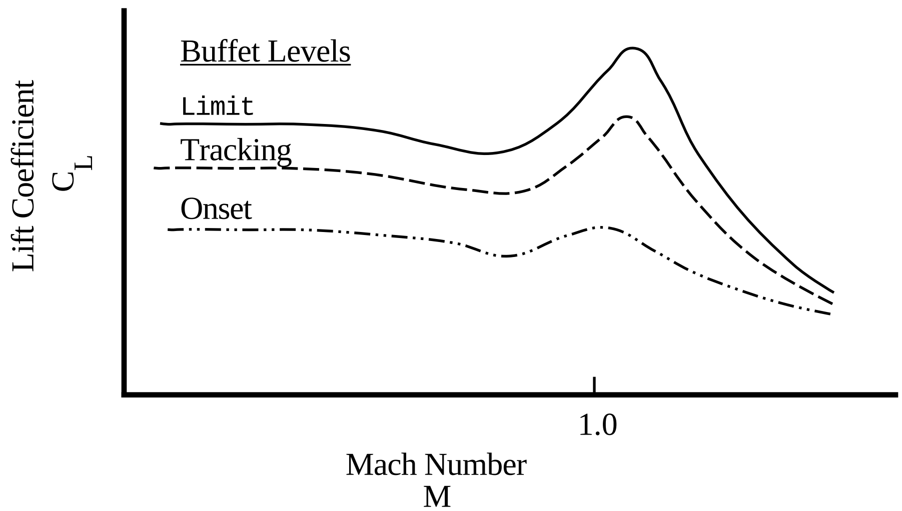

Figure 6.38
LIFT COEFFICIENT VERSUS MACH NUMBER CHARACTERISTICS

From the faired data, the instantaneous n_z versus Mach number for any particular altitude (δ) and weight (W) can be calculated using the expression:

$$n_z = \left(\frac{\delta}{W}\right)\left(0.7\ P_{ssl}\ S\right) C_L M^2 \qquad \text{(Eq 6.69)}$$

Using these values of load factor, instantaneous turn radius, and turn rate can be determined (Section 6.5.2.1). Alternately, instantaneous n_z can be plotted directly on a maneuvering diagram for the altitude of interest.

Another way to obtain instantaneous turn parameters involves Eq 6.69 written in the following form:

$$\left(n_z \frac{W}{\delta}\right)_{Test} = \left(0.7\ P_{ssl}\ S\right) C_L M^2 \qquad \text{(Eq 6.70)}$$

Where:

C_L	Lift coefficient	
δ	Pressure ratio	
M	Mach number	
n_z	Normal acceleration	g
P_{ssl}	Standard sea level pressure	psf

S	Wing area	ft^2
W	Weight	lb.

The left side of this equation is referred n_z; the right side is a function of Mach number. A plot of referred n_z versus Mach number holds data from tests at any weight or altitude. From the referred n_z curve, values of unreferred n_z can be obtained for any desired weight and altitude combination in order to plot instantaneous turn parameters for analysis.This procedure is similar to the other, except there's no need to calculate C_L directly.

6.6.2 STEADY TURN

The steady turn analysis begins with plots of standard day load factor versus Mach number for each test altitude. These plots can be faired to get a smooth variation for the calculation of turn radius and rate using V_T and $n_{z\ Std}$.

Alternately, the smoothed values of $n_{z\ Std}$ can be plotted directly on a maneuvering diagram for the altitude of interest. Values of turn radius and turn rate are simultaneously displayed on the plot.

Once plotted, the sustained turn data can be examined for compliance with mission standards or specifications. In addition, combined sustained and instantaneous turn performance data can be examined with respect to engine-airframe compatibility. Assessments can be made concerning the amount of the available maneuvering envelope beyond the sustained performance capability of the airplane. Areas for potential improvement are depicted in figure 6.39.

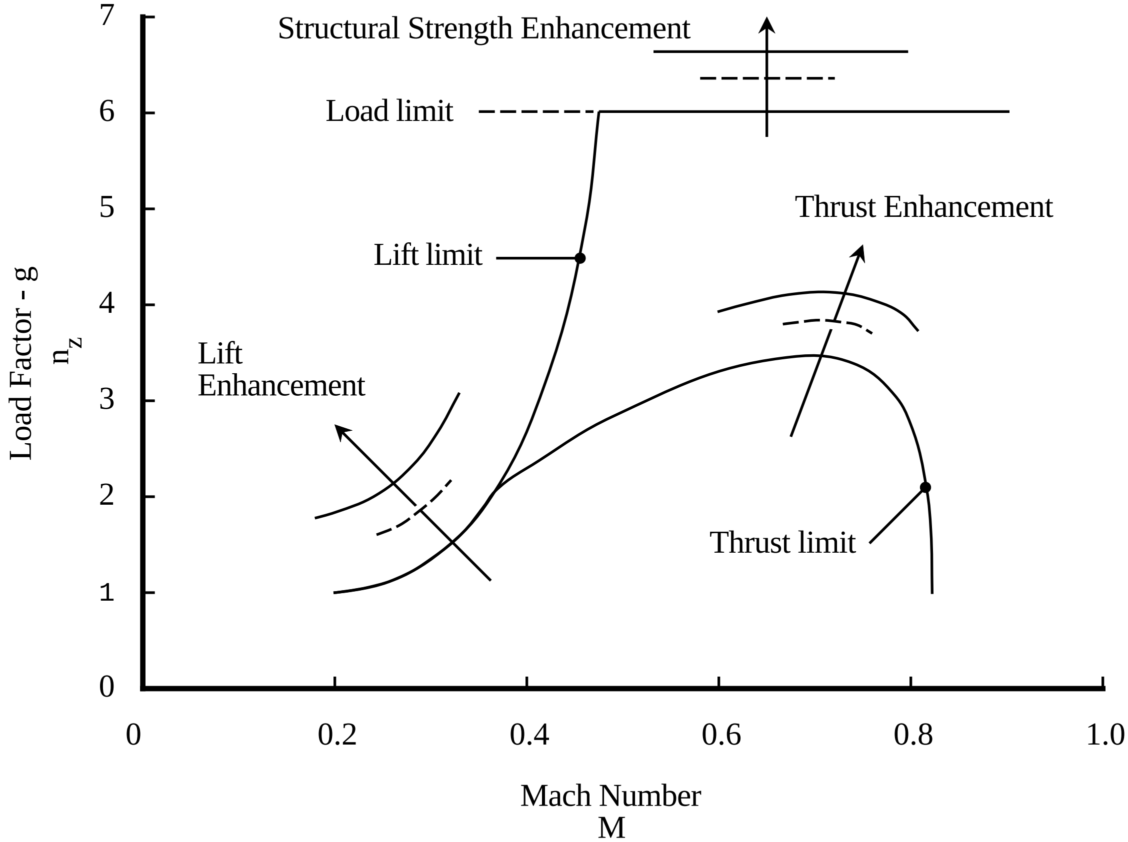

Figure 6.39
ENGINE-AIRFRAME COMPATIBILITY

6.6.3 LOADED ACCELERATION AND DECELERATION

Data from loaded accelerations and decelerations are compiled and added to 1 g acceleration data. These combined data can be plotted in a variety of formats. One example format is a family of curves showing P_S different load factors, as shown in figure 6.40

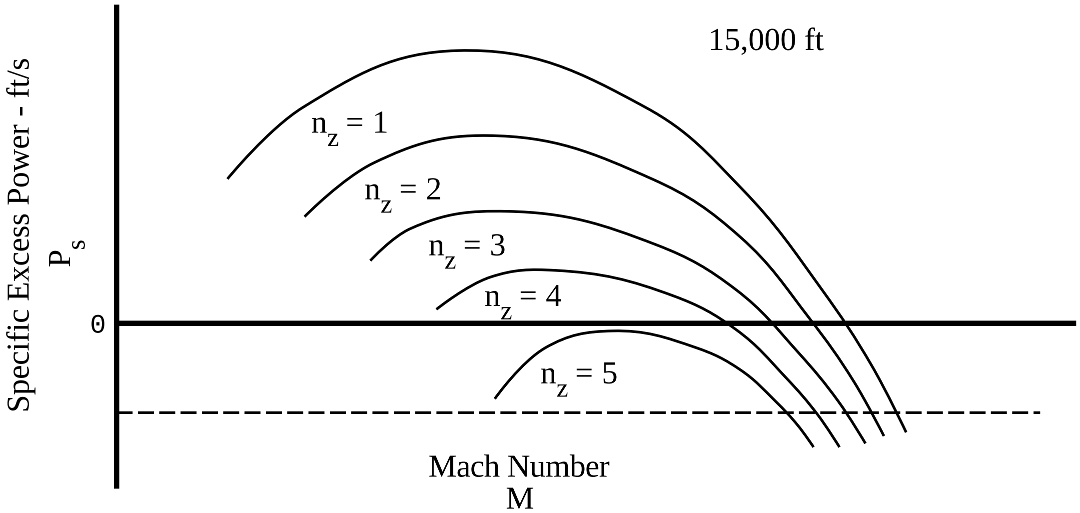

Figure 6.40
SPECIFIC EXCESS POWER VERSUS MACH NUMBER FOR VARIOUS LOAD FACTORS

Horizontal cuts in this plot indicate turn performance at specific values of P_S. For example, the horizontal axis ($P_S = 0$) represents the level sustained turn performance. A cut at a negative P_S can be interpreted as the turn performance that: 1) can be attained while passing through 15,000 ft in a corresponding rate of descent; or 2) will result in a deceleration equivalent to that energy loss rate.

6.6.4 AGILITY TESTS

The analysis for agility test results consists of tabulating the data. Time traces, if available, can provide insights into agility characteristics, but the analysis is largely covered in the flying qualities evaluation. Figure 6.41 show a typical data trace from one of these maneuvers.

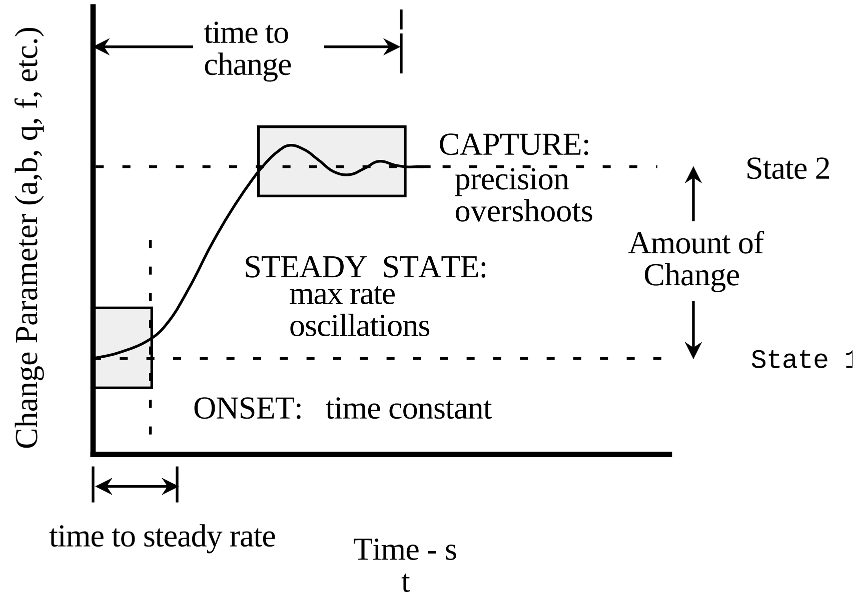

Figure 6.41
AGILITY TEST DATA TRACE

The time to steady rate of change and the time to capture the final steady state are seen in this data trace.

6.7 MISSION SUITABILITY

The mission suitability of the turning performance characteristics of an airplane depends upon its detailed mission requirements. For an airplane with a mission requirement for maneuverability, the turning performance characteristics are evaluated in light of the whole weapons system, in the predicted tactical scenario. The factors affecting the outcome of air-to-air combat are many, as illustrated in figure 6.42.

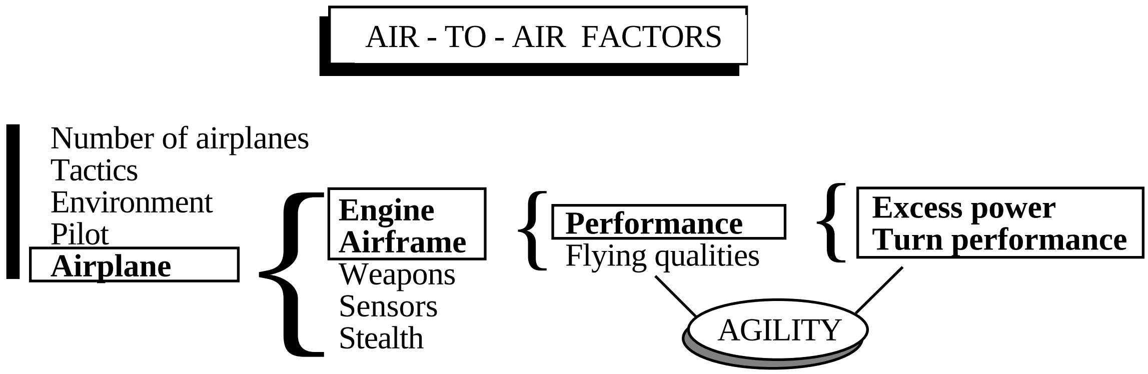

Figure 6.42
FACTORS AFFECTING AIR-TO-AIR COMBAT

Evaluation of each factor listed in the above figure provide data on relative strengths and weaknesses of airplanes, but no one factor guarantees mission success. The turn performance characteristics investigated in this chapter can be used to make comparisons and predictions, but superior performance in this category does not necessarily infer the airplane is better suited for the mission. Nevertheless, it's worthwhile to investigate the common turn performance and agility measures so relative advantages of the airplanes can be placed in the proper perspective.

The chief maneuvering characteristics presented in the previous sections were turn radius, turn rate, and excess energy. There are tradeoffs. High speeds mean high available energy for climbs and turns, giving more available options; however, turn rate and radius suffer, even at high load factors. The advantages of slow speeds are increased turn rate and decreased turn radius; however, at a relatively low energy state, the airplane become susceptible to attack. The relevance of turn performance parameters are discussed below with respect to basic tactical maneuvers.

6.7.1 LOAD FACTOR

While load factor alone does not prescribe turn rate or radius, it describes an airplane limit which is a potential maneuvering restriction. The freedom to use high load factors allows the pilot to maneuver at g levels which may be denied to some adversaries. Specifically, a higher limit load factor is a significant advantage, producing a higher turn rate and forcing an opponent to slow down to match your turn.

While current technology has produced combat airplanes capable of very high load factors and rapid g onset rates, the value of this maneuvering capability depends upon the ability of the pilot to cope with the high g environment. Physiological problems associated with this strenuous high g environment include g-induced loss of situational awareness and g loss of consciousness (G-LOC). These debilitating conditions, the results of rapid onset rates to high load factors, leave the pilot either unable to keep up with the tactical situation or, in extreme cases, unconscious. New anti-g flight equipment is under development to give the pilot the freedom to use the full maneuvering potential of the airplane.

6.7.2 TURN RADIUS

Maximum performance turn radius is largely a function of speed. The really tight turns are made only at low speeds. At the same speed, two opposing airplanes have different turn radii only if they're at different load factors. In that case, their turn rates are different as well and it's difficult to isolate the advantage of a small turn radius. If one of the airplanes is at a lower speed, with equal turn rates, it enjoys a position advantage if both airplanes continue the turn. Consider the one-circle fight depicted in figure 6.43.

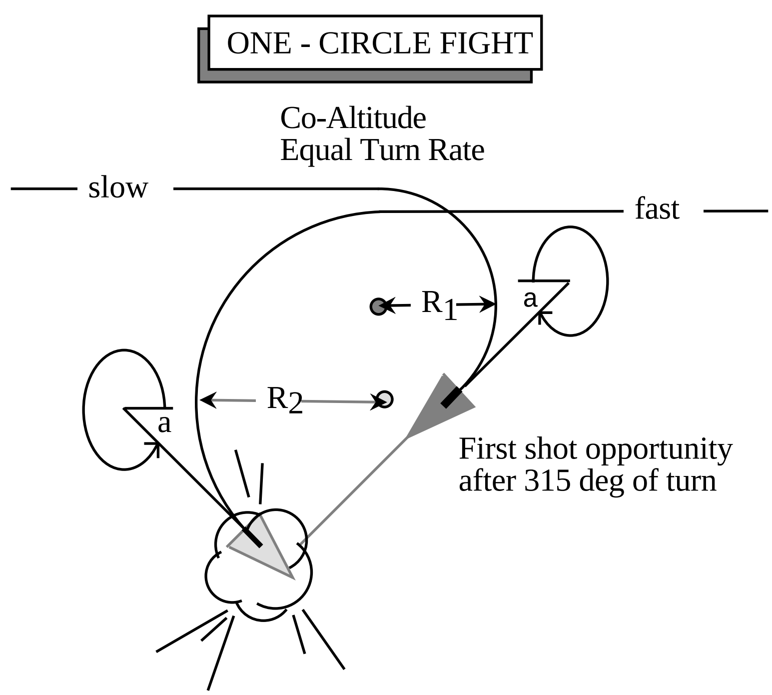

Figure 6.43
TURN RADIUS ADVANTAGE

To employ a forward-firing weapon against an adversary, it is necessary to put the enemy in your forward field of view (also, the weapon's). In the situation depicted above, the smaller turn radius (R_1) forces the opponent out in front. Even if the opponent has turned more degrees, it is still in the slower airplane's field of view due to the geometry of the engagement. If the slow airplane were able to turn as tightly at a faster engaging speed, the shot opportunity comes sooner. The type of weapon employed in this situation affects the outcome, since the fast airplane may have extended beyond the maximum range of the weapon, or may have rotated his nozzles out of the detection envelope of a heat-seeking missile. Still, the position advantage from a small turn radius is seen as the ability to put the opponent in your gun sight first.

Small turn radius confines the maneuvering to a relatively small area, making it easier to maintain visual contact with other airplanes. Formation tactics are enhanced, since it's easier for tactical elements to provide mutual support and to maneuver within the formation.

Turn radius is also relatable to ground attack missions. For straight attacks, the pilot has to be on track, there's no time to search for the target and no flexibility in the attack course. If turns in the target area are permissible, they must be tight turns to allow the pilot to acquire the target and maintain contact with it while prosecuting the attack. If high speeds are warranted in order to maintain a defensive posture while maneuvering in the target area, the required tight turns can be made only with high load factors, complicating the pilot's task.

6.7.3 TURN RATE

The heart of turn performance mission relation is the consideration of turn rate. In almost every tactical situation, turn rate is the measure of maneuvering advantage. When opposing fighters pass head on, the entire focus is on “getting angles”, the process by which a turn rate advantage is exploited to gain an offensive position. The significance of turn rate can be seen in the following depiction of a two-circle fight (Figure 6.44).

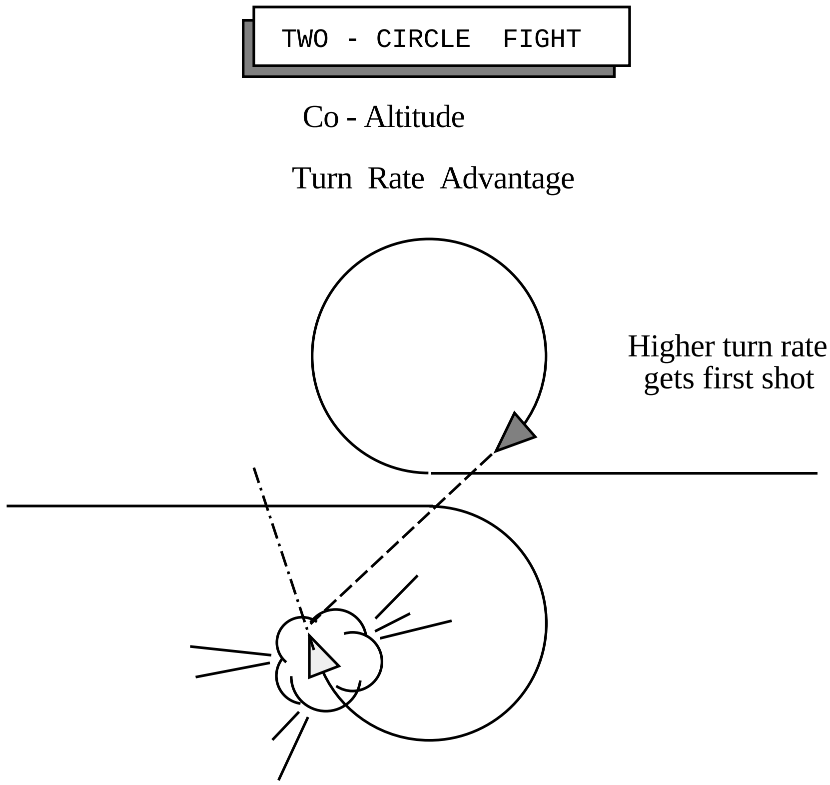

Figure 6.44
TURN RATE ADVANTAGE

A sustained turn rate advantage allows the pilot to put continual pressure on the adversary, eventually producing a shot opportunity or forcing the opponent to make a mistake. The importance of turning quicker encourages pilots to use the vertical plane of maneuvering to take advantage of the increased turn rate during a pull-down from a high relative position. The pilot exploits the tactical egg (Figure 6.7) by using gravity to enhance his turn rate over the top. An instantaneous turn rate advantage can produce the opportunity for a shot, which may justify the high energy loss, as long as it ends the engagement. In these tactical situations, time is critical to both offensive advantage and survivability. Turn rate is the one turn parameter which describes performance against the clock.

6.7.4 AGILITY

6.7.4.1 THE TACTICAL ENVIRONMENT

Missile technology has progressed to the point where the pilot who gets the first shot off will probably win an air-to-air engagement. Following a head-on pass, the first shot will probably be fired within 5 to 10 seconds. In this environment, it's tactically sound to do whatever is necessary to be the first to point at the opponent, even if it means slowing down to take advantage of high instantaneous turn rates. Post-stall maneuvering technology, featuring vectored thrust for pitch and yaw control augmentation, is the focus of much recent interest. This technology is intended to exploit the first-shot constraint by employing extremely rapid decelerations to below the 1 g stall speed. A typical tactical scenario is depicted in figure 6.45.

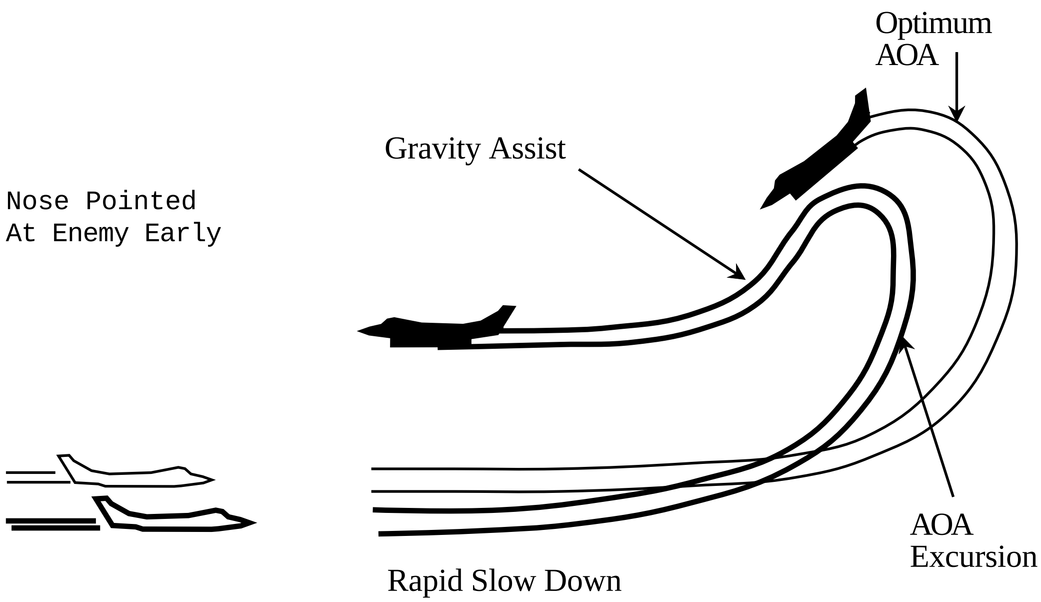

Figure 6.45
QUICK TURNAROUND USING POST-STALL TURN

At these post-stall conditions, very high instantaneous turn rates are possible using vectored thrust against very little aerodynamic damping. The nose is brought around using a combination of pitch and yaw rates to point at the opponent and fire the first shot. Rapid accelerations are performed to regain normal combat energy levels to engage other threats. The pilot uses instantaneous turn rate to rapidly point at his adversary, sacrificing energy to get the first shot, as illustrated in figure 6.46.

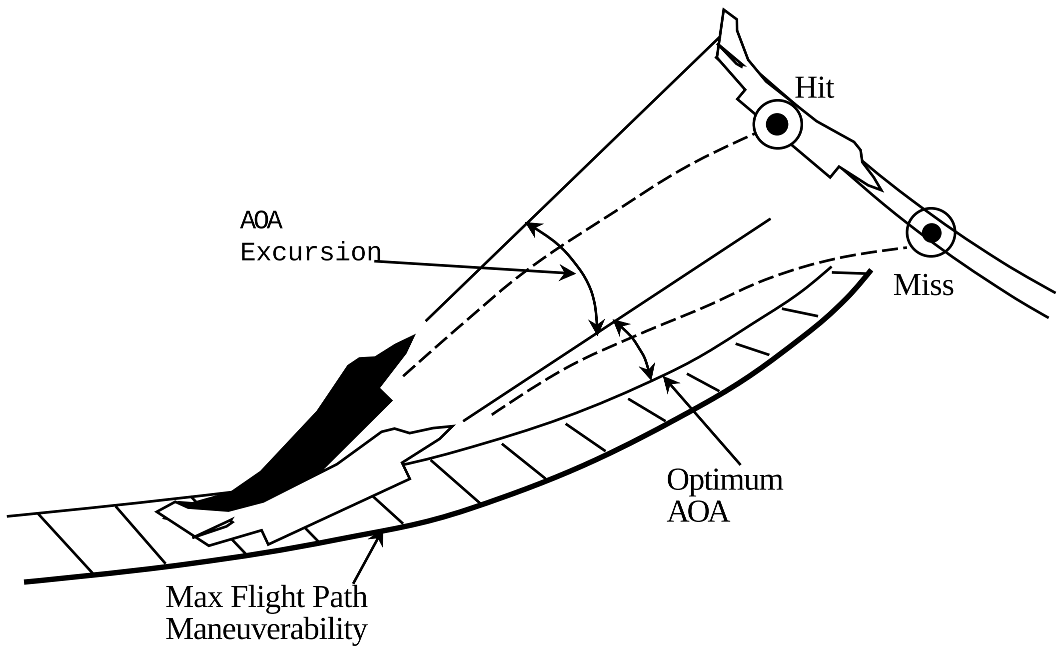

Figure 6.46
RAPID PITCH POINTING

The appeal of this technology is based on the capability to rapidly regain energy using a high thrust-to-weight ratio fighter design.

6.7.4.2 MISSILE PERFORMANCE

A big constraint in air-to-air combat is the requirement to point at the target before firing. This constraint is based largely upon missile capabilities. If the missiles are launched from a trail position at a reasonable range, the missile has very little maneuvering to do. On the other hand, to exploit the post-stall technology mentioned above, missiles have to be launched at very low speeds (high angle of attack), probably at a high angle-off. The missile has to accelerate from a very low speed and then perform a hard turn due to the high angle-off. Missile turn performance is a key issue for these tactics, since to a large extent, the missile is a mini-fighter with a slashing attack capability. As the fighter's requirement for close-in maneuvering diminishes, the demands on the missile increase.

6.7.4.3 DEFENSIVE AGILITY

Agility gives a defensive capability to generate rapid transients to confuse an enemy or to disrupt his attack. Such a defensive situation is depicted in figure 6.47.

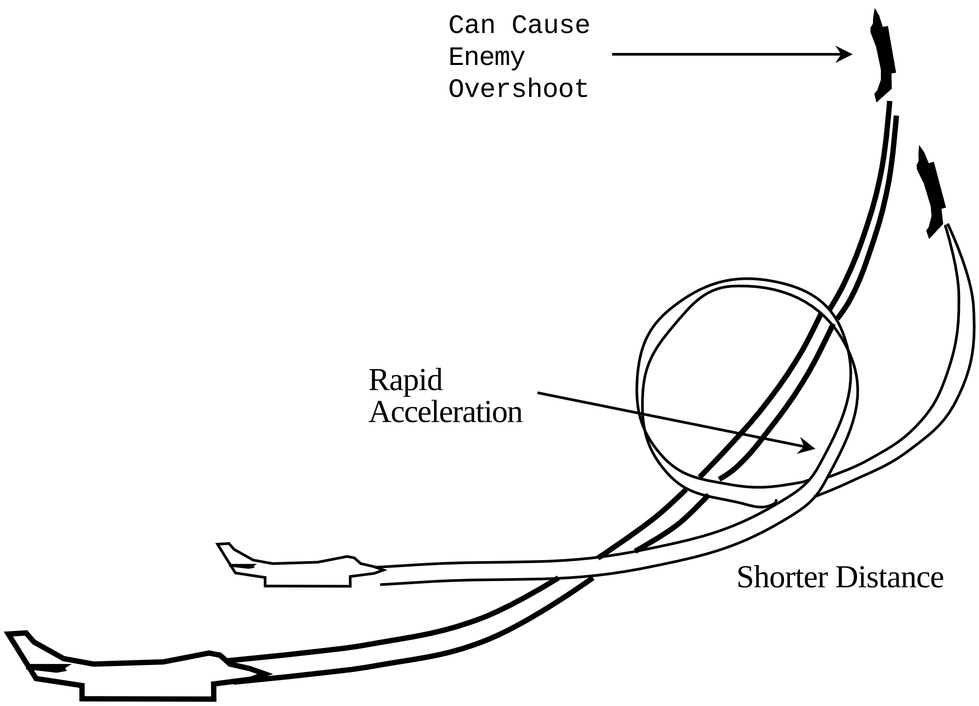

Figure 6.47
DEFENSIVE MANEUVER

This type of maneuver takes away the opponent's immediate offensive advantage, and a capability for rapid acceleration to maneuvering speed evens the odds.

6.7.4.4 CONTROLLABILITY

The previous discussions neglected an important aspect of agility, controllability. In this context, controllability means the ability to control the flight path geometry. The precise attitude control required for aiming is related more to flying qualities than performance. Here, the emphasis is on quick movements, like rapid 180 deg course reversals. From a mission evaluation viewpoint, the ability to start rapid changes in the flight path vector is not particularly useful if the change can't be stopped at the right place. There is no advantage to have a nimble airplane which can’t be controlled. Mission situations demanding more control force the pilot to be less aggressive with the controls. The classic case was the very maneuverable MiG-15 which lost repeatedly to the F-86 because of the Sabre's far superior controllability. Agility demands not only an enhanced maneuverability, but the ability to use it with accuracy.

6.8 SPECIFICATION COMPLIANCE

Standards for agility are in the developing stages, but a sample agility specification might contain turn rate and P_s minimum requirements within a tactical maneuvering corridor, such as:

At 15,000 ft, between 0.4 M and 0.8 M, for a given configuration and loading:

Sustained turn rate:	≥ 12 deg/s
Specific excess power:	≥ 75 ft/s

Another agility specification might address the minimum time to change states. Here, the relevant states are attitude, rate, and flight path acceleration. The specification might address the time from steady state to some threshold rate of change, and the time from initial steady state to final steady state.

6.9 GLOSSARY

6.9.1 NOTATIONS

a	Speed of sound	ft/s
AR	Aspect ratio	
a_R	Radial acceleration	ft/s^2
C_D	Drag coefficient	
C_L	Lift coefficient	
$C_{L_{max}}$	Maximum lift coefficient	
$C_{L_{max_{Test}}}$	Test maximum lift coefficient	
D	Drag	lb
$\Delta H_{P_{ic}}$	Altimeter instrument correction	ft
ΔH_{pos}	Altimeter position error	ft
$\Delta n_{z_{ic}}$	Normal acceleration instrument correction	g
$\Delta n_{z_{tare}}$	Accelerometer tare correction	g

D_{Std}	Standard drag	lb
ΔT	Change in thrust	lb
D_{Test}	Test drag	lb
ΔV_{ic}	Airspeed instrument correction	kn
ΔV_{pos}	Airspeed position error	kn
e	Oswald's efficiency factor	
E_h	Energy height	ft
F_R	Radial force	lb
F_Y	Sideforce	lb
g	Gravitational acceleration	ft/s^2
h	Tapeline altitude	ft
H_P	Pressure altitude	ft
H_{P_c}	Calibrated pressure altitude	ft
H_{P_i}	Indicated pressure altitude	ft
H_{P_o}	Observed pressure altitude	ft
K	Constant	
L	Lift	lb
L_{aero}	Aerodynamic lift	lb
M	Mach number	
M_o	Observed Mach number	
n_L	Limit normal acceleration	g
n_R	Radial load factor, $\frac{F_R}{W}$	g
n_Y	Sideforce load factor, $\frac{F_Y}{W}$	g
n_z	Normal acceleration	g
$n_{z\ sust}$	Sustained normal acceleration	g
$n_{z\ sust\ max}$	Maximum sustained normal acceleration	g
n_{z_i}	Indicated normal acceleration	g
$n_{z_{max}}$	Maximum normal acceleration	g
n_{z_o}	Observed normal acceleration	g
$n_{z_{Std}}$	Standard normal acceleration	g
$n_{z_{Test}}$	Test normal acceleration	g
$\frac{N}{\sqrt{\theta}}$	Referred engine speed	RPM
OAT	Outside air temperature	˚C or ˚K
P_a	Ambient pressure	psf

P_s	Specific excess power	ft/s
$P_{s\ 1\ g}$	Specific excess energy at 1 g	ft/s
P_{ssl}	Standard sea level pressure	2116.217 psf
q	Dynamic pressure	psf
R	Turn radius	ft
$R_{min\ V>V_A}$	Minimum turn radius for $V > V_A$	ft
R_{sust}	Sustained turn radius	ft
S	Wing area	ft^2
T	Thrust	lb
TE	Total energy	ft-lb
T_{ex}	Excess thrust	lb
T_G	Gross thrust	lb
THP_{avail}	Thrust horsepower available	hp
THP_{req}	Thrust horsepower required	hp
T_N	Net thrust	lb
T_{Std}	Standard thrust	lb
V_A	Maneuvering speed	ft/s
V_c	Calibrated airspeed	kn
V_i	Indicated airspeed	kn
V_{max}	Maximum airspeed	kn
V_{min}	Minimum airspeed	kn
V_{mrt}	Military rated thrust airspeed	kn
V_o	Observed airspeed	kn
V_s	Stall speed	kn or ft/s
V_T	True airspeed	ft/s
W	Weight	lb
W_{Std}	Standard weight	lb
W_{Test}	Test weight	lb
n_R	Radial load factor	g

6.9.2 GREEK SYMBOLS

α (alpha)	Angle of attack	deg
α_j	Thrust angle	deg
δ (delta)	Pressure ratio	
δ_h	Pressure ratio for selected altitude	
δ_{Test}	Test pressure ratio	
ϕ (phi)	Bank angle	deg
ϕ_E	Equivalent bank angle	deg
γ (gamma)	Flight path angle	deg
π (pi)	Constant	
ω (omega)	Turn rate	rad/s
$\omega_{max\ V>V_A}$	Maximum turn rate for $V > V_A$	rad/s
ω_{sust}	Sustained turn rate	deg/s

6.10 REFERENCES

1. Hoover, A.D., *Testing for Agility - a Progress Report*, Thirty-Second Symposium Proceedings, Society of Experimental Test Pilots, October, 1988.

2. McAtee, T.P., *Agility - Its Nature and Need in the 1990s*, Thirty-First Symposium Proceedings, Society of Experimental Test Pilots, September, 1987.

3. Naval Test Pilot School Flight Test Manual, *Fixed Wing Performance, Theory and Flight Test Techniques*, USNTPS-FTM-No.104, U. S. Naval Test Pilot School, Patuxent River, MD, July, 1977.

4. Powell, J., *Airplane Performance*, USNTPS Classroom Notes, USNTPS, Patuxent River, MD.

5. Rutowski, E.S., *Energy Approach to the General Aircraft Maneuverability Problem*, Journal of the Aeronautical Sciences, Vol 21, No 3, March 1954.

6. USAF Test Pilot School, *Performance Phase Textbook Volume I*, USAF-TPS-CUR-86-01, USAF, Edwards AFB, CA, April, 1986.